Energy &
Environment Nexus

https://doi.org/10.48130/een-0026-0001

Review

Open Access

Geometric design and application exploration of tubular solid oxide fuel cells

Tong Wang[1#], Yanling Feng[1#], Yeqing Ling[1], Bin Wang[2], Yakun Wang[1], Mohd Hafiz Dzarfan Othman[3*] and Tao Li[1*]

Received: 7 November 2025

Revised: 24 December 2025

Accepted: 12 January 2026

Published online: 28 February 2026

Abstract

Solid oxide fuel cells (SOFCs), as promising and efficient power generation devices, can play an important role in addressing the energy crisis and environmental challenges. Among various cell architectures, tubular SOFCs are distinguished by their exceptional thermal shock resistance and simplified sealing requirements, making them highly suitable for robust long-term operation. This review presents the development status of tubular SOFCs with different geometries, covering the manufacturing methods and stack assembly designs. It is concluded that while conventional tubular designs offer mechanical robustness, flat-tubular geometries provide superior volumetric power density essential for stationary stacks, whereas micro-tubular architectures are uniquely suited for portable applications due to their rapid thermal cycling capabilities. Furthermore, the review outlines the current status of tubular SOFCs integrated with other systems, such as in transportation applications, combined heat and power (CHP) systems, and gas turbines. These integrations demonstrate the potential of tubular SOFCs in promoting sustainable energy utilization. Finally, future development directions are proposed based on the specific characteristics of these tubular configurations.

Keywords: Tubular SOFCs, Geometry design, Fabrication technique, SOFC application

Highlights

- Systematically reviews advanced fabrication techniques for diverse tubular SOFC geometries.
- Critically analyzes state-of-the-art stack designs, assembly strategies, and technical bottlenecks.
- Highlights diverse application scenarios ranging from portable power units to integrated hybrid systems.
- Proposes geometry-specific development roadmaps and future perspectives based on intrinsic cell characteristics.

# Authors contributed equally: Tong Wang and Yanling Feng

* Correspondence: Mohd Hafiz Dzarfan Othman (dzarfan@utm.my); Tao Li (101012902@seu.edu.cn)

Full list of author information is available at the end of the article.

https://doi.org/10.48130/een-0026-0001

Graphical abstract

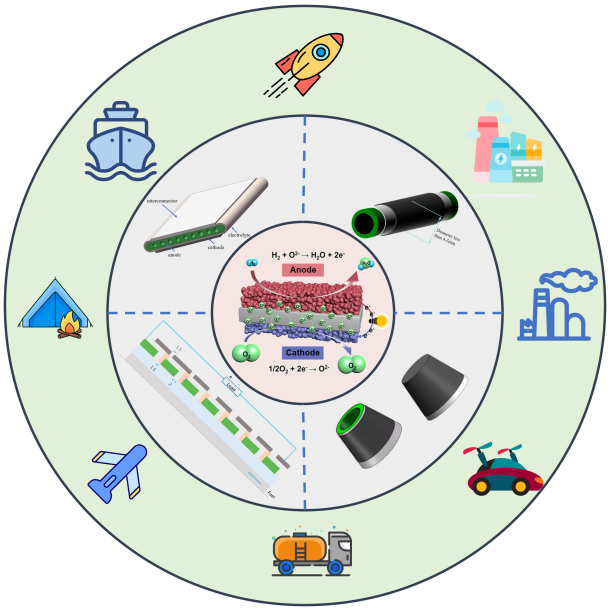

Introduction

Due to the increasing global population and technological advances, the world's energy demand is sharply increasing. Consequently, substantial amounts of pollutants, such as CO_2, CO, and NO_X are emitted into the atmosphere. In response to these environmental challenges, major economies have committed to ambitious climate targets, most notably the 'Carbon Neutrality 2050' initiative. Driven by these global policy frameworks, building highly efficient energy systems and exploring green energy sources are receiving a great deal of attention[1]. Hydrogen is widely accepted as a promising clean energy carrier to achieve carbon neutrality. Fuel cell technology is one of the major routes to convert hydrogen into electricity, with efficiencies unrestricted by the Carnot cycle[2]. Fuel cells can be categorized according to their operating temperatures, with low-temperature fuel cells including proton exchange membrane fuel cells (PEMFCs), alkaline fuel cells (AFCs), and phosphoric acid fuel cells (PAFCs), and high-temperature fuel cells including molten carbonate fuel cells (MCFCs) and solid oxide fuel cells (SOFCs)[3]. Compared with other types, SOFCs display some unique features, such as the generation of high-quality waste heat, improved efficiency, etc.[4,5]. In addition, the high working temperatures (around 700 °C) enable the utilization of numerous fuels, including hydrocarbons, biogas, and ethanol/methanol, thus significantly extending their potential applications[6].

Among various geometries of SOFCs, tubular and planar SOFCs have been most extensively investigated[7], as shown in Fig. 1. At present, commercial SOFCs predominantly adopt planar design[8]. The power level of the planar SOFC stack/system developed by Ceres Power and Hexis reached the kW level and has operated stably for over 10,000 h[9–12]. NASA successfully demonstrated a planar SOFC stack with a power density of 1.37 kW kg^{-1}[13]. However, weak thermal cycling stability and intricate sealing requirements are two major issues that limit the widespread use of planar SOFCs[14]. In contrast, tubular SOFCs are easy to seal and demonstrate robust thermal cycling stability[15]. Additionally, tubular structures feature faster start-up and shut-down, higher mechanical strength, and superior thermal cycling stability[16,17].

Tubular SOFCs emerged in the 1960s[18], and the cathode-supported tubular SOFCs manufactured by Westinghouse were a

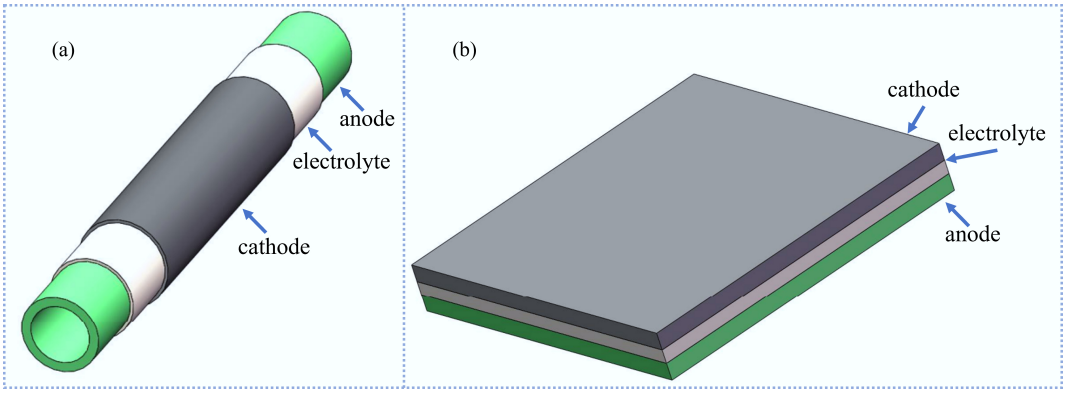

Fig. 1 Schematic of SOFC: (**a**) tubular structure, (**b**) planar structure.

typical representative of the early examples of tubular SOFCs[19]. Although Westinghouse has stopped research on tubular SOFCs, the feasibility and potential of this technology have been well demonstrated through the fabrication of the single cell and systematic testing on both single cells and stacks. Despite a reported operational lifespan beyond 20,000 h[20], the power density of tubular SOFCs remained relatively low owing to inefficiencies in cell stacking and elongated electrical pathways resulting in high cell losses[21]. To improve performance, intense research efforts have focused on exploring novel materials and geometrical designs. State-of-the-art tubular SOFCs have achieved a peak power density of 2 W cm^{-2} (at 700 °C with low calorific value gases)[22], facilitating their adoption in multiple practical fields.

Yet, a systematic overview covering the fabrication, stacking, and application distinctions among different tubular geometries is still limited in the literature. In this review, fabrication methods for single-cell and stack assembly designs are comprehensively described. In addition, practical applications of tubular SOFCs are outlined, such as in transport applications, cogeneration based on tubular SOFCs, integration with gas turbines, and emerging energy technologies. Finally, current challenges to be addressed and future directions are presented.

Geometry of tubular SOFCs

The structural design of tubular SOFCs has undergone significant evolution to enhance mass transport and electrochemical performance. Initially, Westinghouse Electric Corporation fabricated tubular SOFCs by depositing thin layers of cell components on a porous calcia-stabilized zirconia support[23]. Although the porous support tube (PST) allowed air to pass through to the cathode, it still created resistance to the passage of gas. To facilitate the diffusion of air, the thickness of the PST was reduced, and then the PST was replaced with a cathode support tube. The performance of the tubular SOFCs with cathode support was significantly improved. Westinghouse conducted numerous long-term tests of the tubular SOFCs. After 25,000 h of testing, the tubular SOFCs exhibited a performance degradation of approximately 0.1% per 1,000 h. The cell exhibited no mechanical damage or performance loss after conducting over 100 thermal cycles, ranging from 1,000 °C to room temperature[24]. These results were crucial for the commercialization of tubular SOFCs. Meanwhile, a pressure test was carried out on the tubular SOFCs, and the performance was obviously improved under a working pressure of 15 atm. Since Westinghouse proposed the initial generation of tubular SOFCs, researchers have developed various innovative types of tubular SOFCs over the past decades, including flat-tubular SOFC (FT-SOFC), cone-shaped SOFC, segmented-in-series SOFC (SIS-SOFC), and micro-tubular SOFC (MT-SOFC). Each geometry exhibits unique advantages and characteristics. The diversified geometries of tubular SOFCs demonstrate applicability in various scenarios. The timeline for the development of various tubular SOFCs and the schematic diagram of SOFC with various geometries are shown in Fig. 2.

Flat-tubular SOFC

The FT-SOFC represents a strategic structural evolution designed to enhance electrochemical performance by optimizing the current collection path. For instance, building upon the conventional tubular architecture[19], this configuration was developed to maximize volumetric power density while retaining mechanical robustness[4]. The FT-SOFC functions as a hybrid design, combining the sealing advantages of tubular cells with the high active area of planar geometries[28]. The anode generally serves as the support of the FT-SOFC, including multiple fuel flow channels[29], as shown in Fig. 2b. In addition to the circular current on both sides, the ribs between the anode channels exhibit electronic conductivity and provide a short path for current collection. This characteristic of the FT-SOFC results in dramatically reduced ohmic resistance and significantly enhanced power density compared to its traditional tubular counterpart. Structurally, the fuel gas and air are segregated by a dense interconnector film on one side of the cell, which interfaces with the cathode of the adjacent cell to establish a series connection, thus enabling stack assembly.

The single-cell

Extensive research has focused on optimizing the geometric design and fabrication parameters of anode-supported FT-SOFCs to maximize their electrochemical output and structural advantages (Table 1). To effectively exhibit the advantages of the FT-SOFC, Lim et al.[30] conducted a performance comparison of a tubular SOFC and an FT-SOFC with the same NiO-YSZ/YSZ/LSM-YSZ/LSM/LSCF structure prepared by the extrusion method. When the voltage was 0.7 V, the corresponding power density of the tubular SOFC was around 0.21 W cm^{-2}, whereas the FT-SOFC reached 0.39 W cm^{-2} at 750 °C with humidified H_2 as fuel, representing an approximately 85.7% improvement in performance. This was due to the presence of ribs in the anode, shortening the path of current transfer. Suzuki et al.[6] fabricated a micro FT-SOFC with a NiO-YSZ anode as support, ScSZ electrolyte, GDC interlayer, and LSCF-GDC cathode. When 20% H_2 in Ar was used as the fuel, the peak power density of the cell was 0.546 W cm^{-2} at 700 °C. Kim et al.[31] used the extrusion method to fabricate a NiO-YSZ anode support, and then the surface of the support was modified by dip-coating a fine powder-sized NiO-YSZ slurry to make the pores uniformly distributed. The remaining cell components were prepared by dip-coating. The final cell produced a maximum power density of 0.56 W cm^{-2} at 850 °C. Park et al.[32] utilized the extrusion technique to manufacture the anode support. Following pre-sintering, a grinding wheel was used to carve one side of the support to form airflow channels to make assembly simpler. The final cell is shown in Fig. 3a and provided a peak power density of 0.498 W cm^{-2} at 700 °C. Wang et al.[33] utilized the extrusion method to manufacture the anode support, and the cell components were prepared by screen printing. With the structure of Ni-YSZ/YSZ/GDC/LSCF-GDC, the final cell produced a peak power density of 0.539 W cm^{-2} at 750 °C. Yoon et al.[34] compared the performance of an FT-SOFC without and with an interconnector. The schematic diagram of the cell is shown in Fig. 3b. The maximum power density of the FT-SOFC without an interconnector was 0.798 W cm^{-2}. When the cell contains the interconnector, the ohmic impedance increases, resulting in a decrease in performance to 0.566 W cm^{-2}.

In practice, SOFCs face problems such as start-stop cycles, maintenance, and operating temperature changes. Therefore, the redox stability and thermal cycle stability of SOFCs are very important. Guan et al.[35,36] proposed the symmetrical FT-SOFC, as shown in Fig. 3c, which can maintain uniform thermal stress on both sides of the flat tube support to ensure the integrity of the cell. Subsequently, the influence of thermal cycling on cell performance was investigated, and the results indicated that the weak contact between cathode and interconnect was the primary cause of performance degradation[37]. This issue can be mitigated by applying a load on the cathode side, and it was found that the performance of the cell was superior to the initial value. During the durability test of the symmetrical FT-SOFC, a total of 2,030 h of operation was conducted under the conditions of discharging at 28 and 21 A,

https://doi.org/10.48130/een-0026-0001

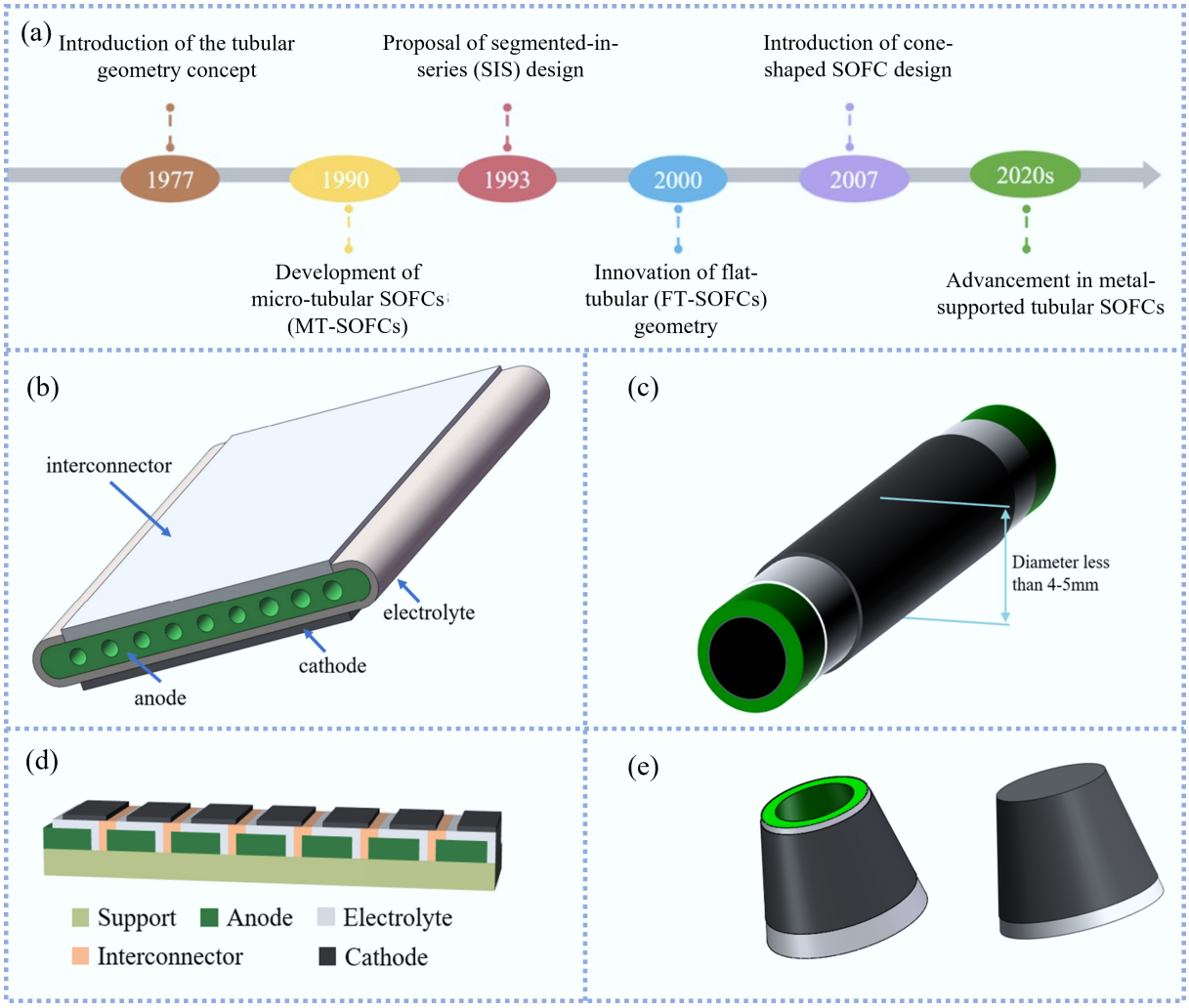

Fig. 2 (**a**) Timeline for the development of various tubular SOFCs[4,25–27]. (**b**) Schematic diagram of the FT-SOFC. (**c**) Schematic diagram of the MT-SOFC. (**d**) Schematic diagram of the SIS-SOFC. (**e**) The schematic diagram of the cone-shaped SOFC.

Table 1 Comparison of peak power densities and geometric parameters of anode-supported FT-SOFCs reported in recent literature

Type	Cell composition	Maximum power density (W cm^{-2})	Test temperature (°C)	Ref.
FT-SOFC	NiO-YSZ/YSZ/LSM-YSZ/LSM/LSCF	0.39	750	[30]
FT-SOFC	NiO-YSZ/ScSZ/GDC/ LSCF-GDC	0.546	700	[6]
FT-SOFC	NiO-YSZ/YSZ/LSCF-GDC	0.498	700	[32]
FT-SOFC	Ni-YSZ/YSZ/GDC/LSCF-GDC	0.539	750	[33]
FT-SOFC	NiO-YSZ/YSZ/LSM-YSZ	0.798	750	[34]

and the performance dropped by about 20%[38]. Khan et al.[39] studied the degradation behavior of an FT-SOFC during long-term operation at constant current densities, which was evaluated through voltage loss. The results showed that operating at high current densities can result in accelerated degradation due to enhanced Ni particles coarsening in the anode, the formation of an insulating phase between cathode and electrolyte, and the evolution of fine particles in the cathode. Therefore, discharging at low current density was a better choice to ensure the stable operation of the cell.

FT-SOFC stacks

Overall, recent progress in FT-SOFC stack development has focused on scaling up cell number and active area while innovating interconnection and sealing architectures, enabling peak stack power to increase from the sub-kW level to ~1 kW at 700–750 °C, albeit sometimes at the expense of volumetric power density. Lim et al.[40] fabricated an FT-SOFC stack consisting of 24 cells, producing a peak power output of 507 W. On this basis, a stack design in which two single cells were connected in parallel into a unit bundle was proposed and verified for further scale-up, as shown in Fig. 4a[30]. Subsequently, a stack with an active area of 5,400 cm^2 was assembled, as shown in Fig. 4b, producing 921 W peak power output at 750 °C using humidified H_2 as fuel[30]. The stack manufactured by Ji et al.[41] was composed of FeCrAl metal flat boxes and five cells were located on the surface of a metal box, which was sealed to the metal box through Ag-Cu air brazing, as shown in Fig. 4c. The final stack produced a peak output power of 614 W. This method provided a new idea for fabricating an FT-SOFC stack, but it leads to a degradation in the

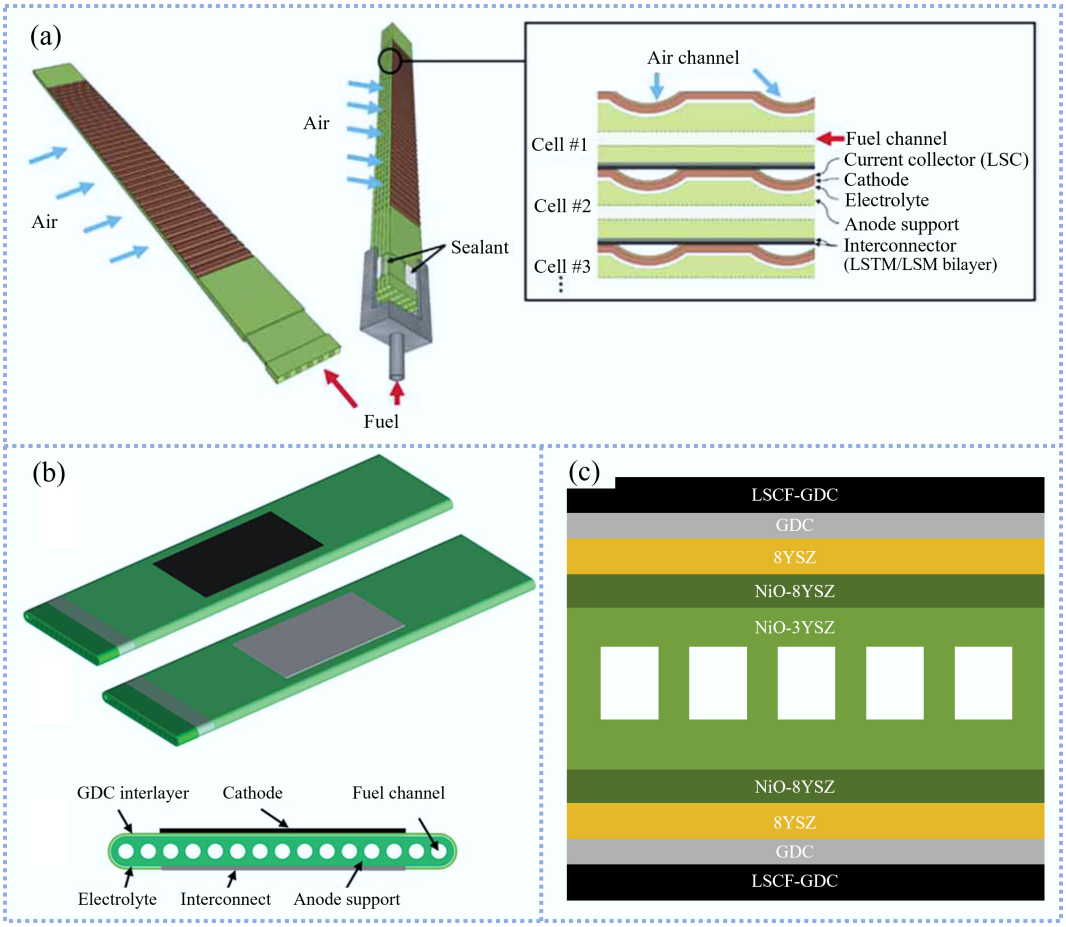

Fig. 3 (**a**) Schematic diagram of the FT-SOFC integrated electrode and air channel[29]. (**b**) Schematic diagram of the FT-SOFC[29]. (**c**) Schematic diagram of the symmetrical FT-SOFC.

volumetric power density of the stack. Park et al.[32] prepared an FT-SOFC stack consisting of five of the monolithic electrodes and gas channels assembly cells. The innovative design enabled single cells to be assembled into stacks like planar SOFCs, which can shorten the current path. The stack achieved a peak output power of 46.2 W. Choi et al.[42] utilized metallic components to assemble a 30-cell stack with a 3,000 cm^2 active area, as shown in Fig. 4d. The metallic components not only functioned to maintain mechanical integrity but also helped with stack sealing. The power output of the stack reached 1 kW at 700 °C. Han et al.[43] investigated the effects of constant-current/constant-voltage discharge on stack performance using a three-cell stack with an active area of 180 cm^2, and a peak power of 103.5 W was obtained at 750 °C. The results indicated that the degradation rate of the stack performance was lower when the stack was operated in constant-current operation mode.

Cone-shaped SOFC

In pursuit of attaining a higher voltage within a limited space, Sui & Liu first proposed the concept of the cone-shaped SOFC, as shown in Fig. 2e[27]. In this innovative design, one cell is fitted into the following cell to form a tubular self-supporting structure[27]. Therefore, the cone-shaped SOFC can be considered as an improved tubular SOFC, retaining the structural characteristics of the tubular design while providing elevated thermal stability[28]. In this design, the interconnect is positioned between the anode of one cell and the cathode of the subsequent one, functioning as both a sealing and an electrical connection. During stack assembly, the substantial quantity of cone-shaped SOFCs makes connection sealing a notable challenge in this design. During stack operation, the fuel flows from the interior of one cell to the interior of the subsequent one, while the air flows on the exterior.

Sui et al.[27] utilized the slip casting technique to prepare a YSZ electrolyte support. The NiO-GDC anode and LSCF-GDC cathode were deposited on the inner and outer sides of the electrolyte support, respectively. The three-cell stack with an active area of 15.9 cm^2 produced a peak power of 0.9 W at 800 °C. Subsequently, Sui et al.[44,45] prepared a 0.196 mm-thick SDC electrolyte support and a 0.26 mm-thick GDC electrolyte support by slip casting, and the final cells produced a peak power density of 0.297 and 0.3 W cm^{-2} at 700 °C, respectively. In general, the performance was not as good as the tubular counterpart due to a thicker electrolyte, resulting in larger ohmic losses. In order to overcome this problem, Zhang et al.[46] utilized slip casting technology to prepare a cone-shaped anode tube, and then a 20 μm-thick YSZ electrolyte was fabricated by dip-coating technology. The ohmic losses from the thin electrolyte membrane were negligible, and the final cell reached a peak power density of 1.15 W cm^{-2} (at 850 °C with moist hydrogen). Bai et al.[47] used dip-coating technology to fabricate a cone-shaped SOFC anode support and a 35.9 μm-thick YSZ electrolyte. The cell achieved a peak power density of 1.35 W cm^{-2} at 850 °C with moist hydrogen. The fabricated stack consisting of two cells with an active area of 11.6 cm^2 produced a peak power of 3.7 W at 800 °C. Ding et

https://doi.org/10.48130/een-0026-0001

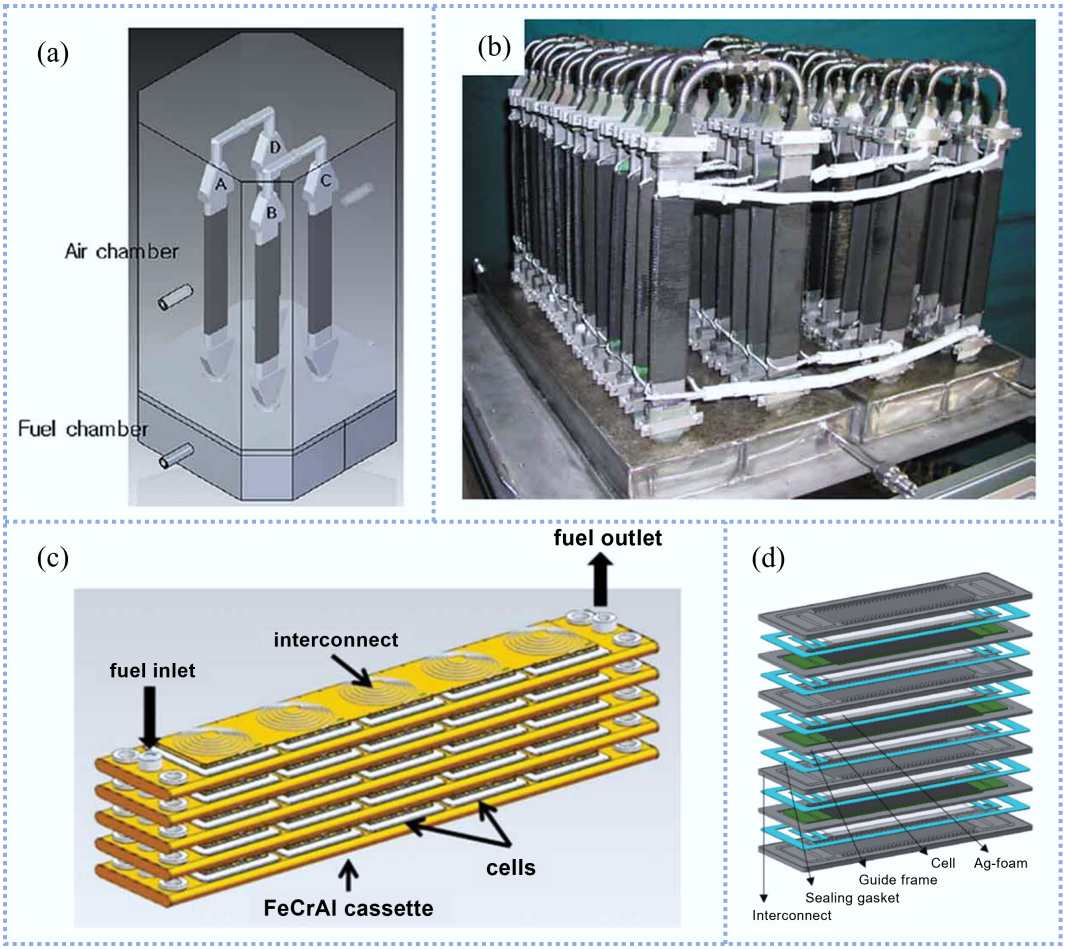

Fig. 4 (**a**) Schematic diagram of a two-unit bundle containing four cells, and (**b**) actual image of the 1 kW class FT-SOFC stack[29]. (**c**) Schematic diagram of stack structure[29]. (**d**) Schematic diagram of the stack components[42]. (Reprinted with permission from Han et al.[43]. Copyright [2022] Elsevier B.V.)

al.[48] utilized the slip casting technique to prepare a NiO-YSZ anode substrate; the NiO-YSZ functional layer and a 6.67 μm-thick YSZ electrolyte film were fabricated by the dip-coating method. The final cell exhibited a peak power density of 1.78 W cm^{-2} at 800 °C. On this basis, the maximum power of the two-cell stack with an active area of 10.65 cm^2 exceeded 2.75 W at 800 °C and showed superior thermal cycling stability. It can be concluded that the utilization of an anode support enables a reduction in electrolyte thickness, consequently enhancing the cell performance. Ding & Liu[49] also used a one-step co-sintering process to manufacture a cone-shaped SOFC, reaching a peak power density of 0.797 W cm^{-2} at 850 °C. The co-sintering method greatly reduces the preparation process and fabrication costs.

The process of fabricating anode support by the slip casting method is complex, while the dip-coating method is time-consuming. In comparison, the gel injection molding technique is a superior alternative. Liu et al.[50] used the gel-casting technique to prepare the cone-shaped anode support, which can obviously reduce cell production time. The final cell produced a peak power density of 0.9 W cm^{-2} at 800 °C. On this basis, the four-cell stack with an active area of 16.2 cm^2 produced a peak output power of 3.4 W at 800 °C. In addition to the above-mentioned technologies, low-pressure injection molding technology[51] and the phase inversion method[52] can also be used to manufacture the cone-shaped SOFCs.

Segmented-in-series SOFC

In recent years, large-scale hybrid power systems based on SOFC technology have been developed. The hybrid system requires a high voltage during operation, but the output voltage that a cell can provide during regular operation is around 0.7–0.8 V, which is far less than the voltage required by the system. To meet the voltage required by the system, multiple cells need to be connected in series, which is a complicated process. SIS-SOFC integrates multiple cells onto a support, which can obtain high output voltage at low current, further reducing ohmic loss[53]. Rolls-Royce initially proposed the concept of segmented-in-series SOFC (SIS-SOFC)[54], The schematic diagram of SIS-SOFC is shown in Fig. 2d. SIS-SOFC includes tubular and flat tubular designs. This geometry structure can provide many advantages, such as: (1) high resistance to redox cycles from ceramic supports; (2) simple sealing; (3) no additional components required with integrated interconnect[55,56].

The extrusion method is a widely used method for fabricating flat tube supports, Mushtaq et al.[57] used the extrusion method to fabricate a 3YSZ flat tube as support, and the cell components were prepared by screen printing and dip-coating. The detailed preparation process is shown in Fig. 5a. The cell with varying cathode thicknesses exhibited different electrochemical properties, and the optimal performance of the SIS-SOFCs composed of five cells was 0.498 W cm^{-2} obtained at a cathode thickness of 57 μm. Kim et al.[58] used the same method to fabricate the SIS-SOFC. The peak power

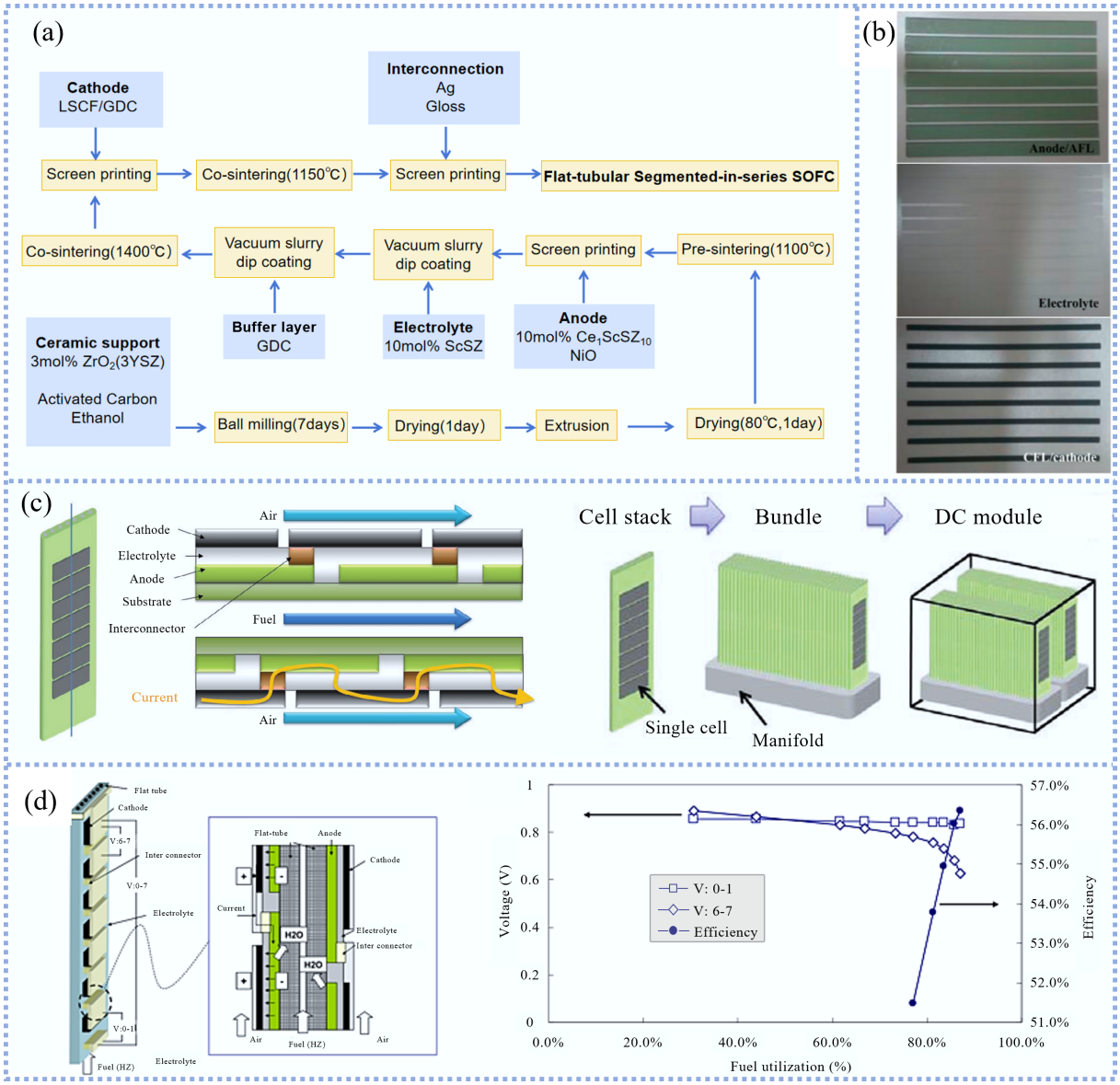

Fig. 5 (**a**) Process of preparing SIS-SOFC. (**b**) Cell components fabricated by decalcomania papers method[61]. (**c**) Schematic of the tubular SIS-SOFC and the stack with 56 tubular SIS-SOFCs[29]. (**d**) Schematic diagram of the SIS-SOFCs stacks consist of 14 cells, and the influence of fuel utilization on voltage. V: 0–1 and V: 6, 7 represent the voltage of the cell at the most upstream and most downstream cell, respectively[68].

density and peak output power of the five-cell unit bundle were 0.618 W cm^{-2} and 2.47 W, respectively. Fujita et al.[59] fabricated an SIS-SOFC with a flat tube support. The cell comprised Ni-doped MgO-based support, NiO-YSZ anode, YSZ electrolyte, and LSCF cathode. With reformed methane used as fuel, the average power density of the SIS-SOFC was 0.195 W cm^{-2} at 0.24 A cm^{-2}. A total of 20 redox cycles were conducted, with only 0.15% performance loss per cycle despite supplying air directly as the oxidant to the anode side. The excellent redox tolerance was due to the fact that the substrate can prevent the diffusion of oxygen, and the presence of Ni in the substrate prevents the anode from being oxidized. Later, Fujita et al.[60] reported that the Ni-doped MgO-based support of SIS-SOFC can prevent the deformation of the cell and thus exhibit high redox tolerance.

In addition to the above mainstream methods, An et al.[61] used the extrusion method to prepare a YSZ support, and the cell components were fabricated by the decalcomania paper methodology, as shown in Fig. 5b. This method allowed the preparation of SIS-SOFCs on all sides of the support, and the thickness and shape of the components can be controlled. The peak power density of the two-cell stack was 0.437 W cm^{-2} at 800 °C. Pillai et al.[62] fabricated a PSZ flat tube support by the gel-casting method, and cell components were prepared by screen printing. The final cell produced a peak power density of 0.7 W cm^{-2} at 800 °C. Kim et al.[63] utilized a direct-writing technique based on selective paste dispensing to prepare cell components on a PSZ support. Compared with traditional methods, this method can improve control over the microstructure. The two-cell SIS-SOFCs produced a peak power of 35 mW at 800 °C at an anode-cathode overlap area of 0.5 cm × 0.1 cm. The open circuit voltage was lower than the theoretical value due to the presence of pores in the interconnects. To address this issue, double-layer interconnects and Ag-glass interconnects have been studied and demonstrated reliable sealing performance[56,64,65]. Zhang et al.[53] used thermal spraying to fabricate SIS-SOFC on an end-close

https://doi.org/10.48130/een-0026-0001

tubular support as shown in Fig. 5c. The dense interconnectors in the closed section of the support can act as a seal, and the open end was in a relatively low-temperature region during operation, making sealing easier. The optimal value of the quantity of cells in series was determined through theoretical analysis. On this basis, a tubular support with an inner diameter of 21 mm was manufactured with 20 cells connected in series. Subsequently, as shown in Fig. 5c, a stack composed of 56 SIS-SOFCs was fabricated and the output power of the stack exceeded 800 W at 830 °C.

Additionally, several companies have conducted research and experimental tests on SIS-SOFC. Mitsubishi Hitachi Power Systems (MHPS)[66] fabricated an SIS-SOFC stack that exhibited excellent stability performance. Operating under normal pressure for more than 7,000 h, the degradation rate per 1,000 h was less than 0.25%. Based on this work, an integrated system with a micro-turbine was developed. Tokyo Gas and its partner company[55] developed a SIS-SOFC stack with an output power of more than 400 W, with a cell degradation rate of approximately 0.31% per 1,000 h. Kyocera Corporation (Japan) conducted a 100,000-h durability test on an FT-SOFC, which was the longest test to date[67]. The performance gradually degraded without sudden changes.

For SIS-SOFCs, multiple cells are arranged on a substrate and the cells located at the upstream consume fuel, resulting in low fuel density for downstream cells, which negatively affects the downstream cells. Koi et al.[68] manufactured SIS-SOFCs consisting of 14 single cells. The cells were divided into two groups on both sides of the insulating substrate with the structure of NiO-YSZ/YSZ/LSCF, as shown in Fig. 5d. With high fuel utilization, the voltage of downstream cells was significantly lower than that of upstream cells. To solve this problem, Cui et al.[69] established a model of SIS-SOFC to optimize the voltage distribution. The simulation results demonstrated that with the active area of the cell gradually increasing along the flow direction of fuel, the downstream cells can maintain a higher voltage under the same current operation. Therefore, this method can alleviate the problem of voltage non-uniformity. Fan et al.[70] set up heat pipes to transfer heat from high-temperature regions to low-temperature regions to diminish the temperature gradient of the cell. Based on the calculation formula of open circuit voltage, it can be concluded that reducing the temperature gradient can alleviate the problem of voltage nonuniformity.

Micro-tubular SOFC

Compared with the traditional tubular SOFC, the micro-tubular design exhibits a higher power density per unit volume, rapid start-up and shut-down and high thermal shock resistance[23,71]. Therefore, MT-SOFC has received widespread attention during the past decades. MT-SOFC was initially reported by Kevin Kendall at the beginning of the 1990s[26]. Essentially, as shown in Fig. 2c, MT-SOFCs can be considered as the miniaturization of traditional tubular SOFCs to the millimeter scale, typically around 5 mm. Hence, MT-SOFC is a preferred choice for portable devices. The design of the microtubular structure proves effective in significantly increasing the specific surface area. Nevertheless, the small diameter of the micro-tube poses challenges for current collection and stack assembly. Despite this challenge, researchers have successfully demonstrated the feasibility and great potential of this state-of-the-art design.

The single-cell

The first generation MT-SOFC mainly used the electrolyte layer as support[26]. However, the thick electrolyte layer led to significant ohmic resistance that limited performance. Subsequently, the anode-supported design had become widely adopted since the thickness of the electrolyte layer could be dramatically decreased down to < 10 μm to achieve high-performance.

The classic process for fabricating anode support by the extrusion method is to mix ceramic powder, polymer and a pore-forming agent into a slurry, and then the slurry is extruded from the mold using an extruder to prepare the anode support. Suzuki et al.[72] fabricated an MT-SOFC by the extrusion method; the porosity of the anode before reduction was approximately 30%. With a structure of NiO-GDC/GDC/LSCF-GDC, the cell produced a peak power density of 0.857 W cm^{-2} at 550 °C. The porosity of the anode can affect the mass transfer capacity of fuel gas. Especially at high gas flow rates, the porosity has a significant effect on cell performance[73]. To increase the porosity of the anode, polymethyl methacrylate beads were incorporated into the anode slurry, which increased the porosity to 46% before reduction, and the pores diameters were evenly distributed[74]. An Ag wire was used to collect current from the electrodes, where the current collection from the anode was only from the edge of the anode tube. The cell produced a peak power density of 1.017 W cm^{-2} at 550 °C. Collecting current from the edges of the tube led to a loss of current collection, Sin et al.[75] positioned the current collecting wires throughout the anode tube. The final cell produced a peak power density of 1.31 W cm^{-2} at 550 °C. Calise et al.[76] used a similar process to fabricate an MT-SOFC, which was tested vertically to overcome non-uniform distribution of fuel gas due to gravity. The cell produced a peak power density of 1.31 W cm^{-2}. With the improvement of the fabrication process, the performance of MT-SOFC manufactured by the extrusion method has gradually improved, which illustrated the applicability of the extrusion method in the MT-SOFC manufacturing process.

The extrusion method allows the fabrication of multilayer structures of MT-SOFC in a one-step process. Kendall[71] reported the fabrication of electrolyte-supported MT-SOFC through the co-extrusion technique. Sun et al.[77] successfully fabricated a NiO-YSZ/YSZ dual-layer micro-tube through thermoplastic co-extrusion. The outer diameter of the tube can be adjusted in the range of 0.4–1.8 mm. Simultaneously, as the diameter of the tube decreased, the thickness of the electrolyte became thinner while maintaining density. Rahman et al.[78] fabricated an MT-SOFC with a diameter of 4.2 mm using the co-extrusion method. The manufacturing process and the actual images of MT-SOFC with seven cells are shown in Fig. 6a. The tube can be viewed as an assembly of seven cells, with the outer layer as anode, the YSZ electrolyte and LSM cathodes were deposited on the interior surface of the seven channels. Mani et al.[79] designed a co-extruder capable of simultaneously fabricating a five-layer structure. The multi-layer anode was segmented into four layers with different nickel content. Unfortunately, the performances of the above-mentioned MT-SOFCs manufactured through the co-extrusion method are not reported, making it uncertain to assess the applicability of the co-extrusion method in MT-SOFC manufacturing.

Aside from ram extrusion, the phase inversion-assisted extrusion method has proven to be a promising alternative for MT-SOFCs manufacturing. Compared to the conventional ram extrusion, the phase inversion method allows for flexible control and tailoring of the micro-structure of ceramic tubes. The phase inversion method was initially utilized to manufacture polymer membranes[80]. Tan et al.[81] first reported the application of the phase inversion method to manufacture ceramic membranes in 2001. Wei & Li[82] utilized the phase inversion method to prepare YSZ hollow fiber membranes as support for MT-SOFC, which featured a typical asymmetric structure. The finger-like structure near the inner surface increased the area loaded with Ni, while the sponge-like structure near the outer

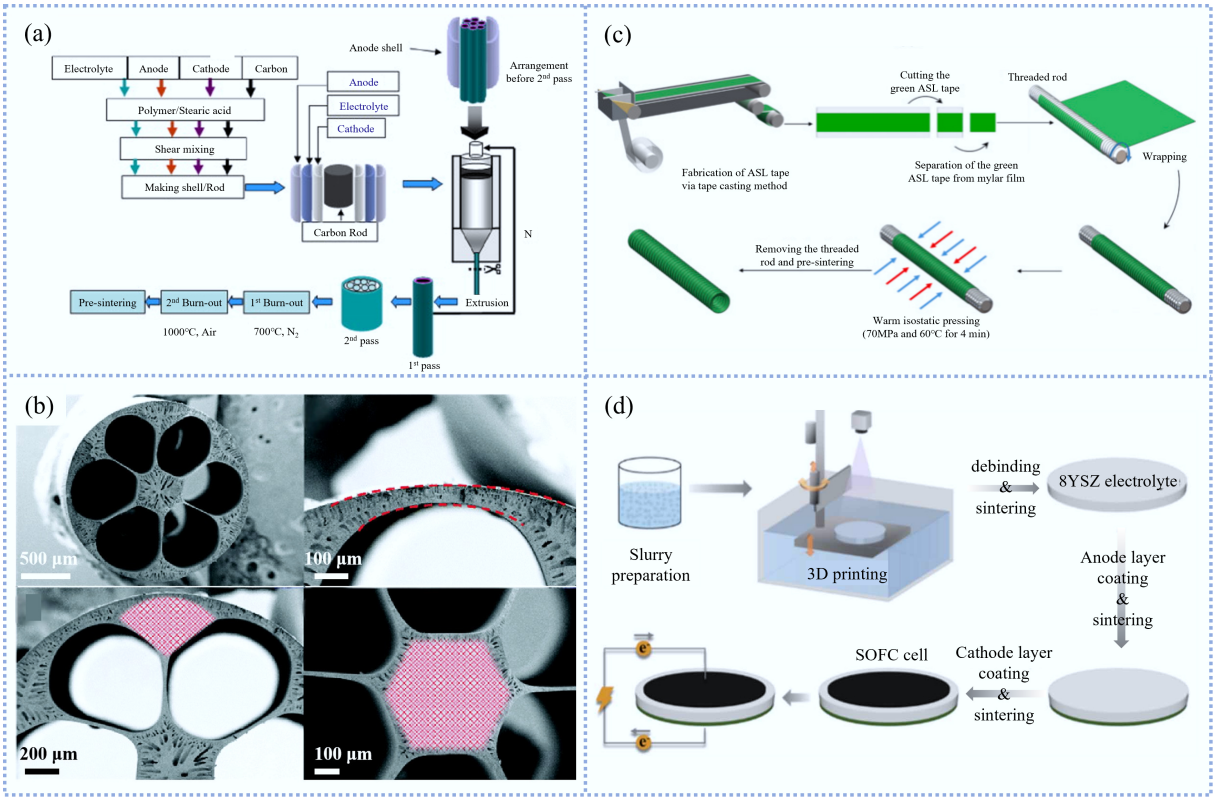

Fig. 6 (**a**) Fabricating process of multi-tubular SOFC with seven cells[78] (Reprinted with permission from Mani et al.[79]. Copyright [2010] Elsevier B.V.). (**b**) SEM photomicrographs of 6-channel anode supports[22]. (**c**) Fabrication steps of anode support bolt-microtube[83] (Reprinted with permission from Kim & Jang[84]. Copyright [2023] Elsevier B.V.). (**d**) Schematic of 3D printed MT-SOFC fabrication process[84].

surface becomes completely dense after sintering, ensuring excellent gas tightness. However, due to the YSZ dense layer thickness reaching 120 μm, resulting in high ohmic loss and only a maximum power density of 0.018 W cm^{-2} was obtained at 800 °C. Therefore, most researchers turned attention to anode-supported hollow fiber MT-SOFC.

Droushiotis et al.[85] used the phase inversion method to prepare a NiO-YSZ anode and found that the mechanical property of the hollow fiber membranes dropped with rising Ni content. Othman et al.[86] investigated eight types of the anode with different lengths of finger-like layers. The result showed that a long finger-like layer enhanced gas diffusion but reduced the electrical conductivity and bending strength of the membrane. Thus, it was evident that the configuration of finger-like layers in the anode had an obvious impact on the overall anode performance. Chen et al.[87] utilized a graphite-assisted phase inversion method to prepare a NiO-YSZ anode with a porosity gradient to alleviate the concentration polarization at high current density. Compared with the original cell, the optimized cell exhibited enhanced electrochemical performance, with the peak power density increasing from 0.51 to 0.66 W cm^{-2} at 850 °C. Notably, concentration polarization had been significantly mitigated at high current density. Yang et al.[88] utilized the phase inversion method to fabricate a Ni-YSZ anode with dual pore structures. The exterior region of the anode, adjacent to the YSZ electrolyte layer, had small finger-like pores, which were regarded as the site of electrochemical reactions. Meanwhile, large finger-like pores on the interior contribute to enhancing fuel gas transfer. The final cell produced a maximum power density of 0.78 W cm^{-2} at 800 °C. Li et al.[22] fabricated the multi-channel MT-SOFC using the phase inversion method, as shown in Fig. 6b. This innovative structure enabled MT-SOFC to exhibit outstanding mechanical robustness compared to single-channel MT-SOFC. Unlike the traditional structure, this structure distributed the support between electrochemically active regions and the central area, reducing the mass transfer resistance. According to the nitrogen permeation results, the multi-channel anode demonstrated superior gas transport capabilities compared to the single-channel structure[8]. The fabricated six-channel MT-SOFC with the structure of NiO-YSZ/YSZ/GDC/LSCF-GDC, reached a peak power density of 2.27 W cm^{-2} at 700 °C. Through optimizing the manufacturing process, Wang et al.[89] optimized the shape of the multi-channel to the tear-drop design. The novel structure further enhanced the mass transfer capability. However, this structure may reduce electrochemical reaction sites, hence the presence of an anode functional layer may be necessary.

Similarly, the phase inversion method allows the simultaneous preparation of multi-layer structures. Li et al.[90] fabricated a NiO-CGO (weight ratio 3:2) anode, a NiO-CGO (weight ratio 2:3) anode functional layer, and a CGO electrolyte using a triple-layer co-extrusion method. The influence of the thickness of the anode functional layer on cell performance was investigated, and the results indicated that a thicker anode functional layer can increase the mechanical robustness of the cell but affects the diffusion of fuel gases, resulting in a degradation of electrochemical performance. Rahman et al.[17] utilized a phase inversion-assisted co-extrusion method to manufacture MT-SOFC with NiO-YSZ/YSZ/LSM-YSZ in one step. Due to the different sintering characteristics of cell components, sintering at high temperatures will lead to a decline in cathode porosity. To solve this problem, YSZ powders with different

https://doi.org/10.48130/een-0026-0001

particle sizes were used to manufacture different structures, and the ideal microstructure was obtained by adjusting the sintering temperature and heating rate. The maximum power density of the final cell was 0.75 W cm^{-2} at 700 °C.

Apart from the above-mentioned mainstream MT-SOFC manufacturing methods, there are also some other methods. Altan et al.[83] proposed the concept of bolt-microtubular SOFC and the fabrication process is shown in Fig. 6c. An anode support with unique patterns was fabricated on the threaded rod by tape casting combined with isostatic pressing, which increased the interface area between the electrode and electrolyte and provided more reaction sites. Simultaneously, the presence of the thread structure was helpful for the current collection through the winding of Ag wire. The final cell produced a peak power density of 0.293 W cm^{-2} at 800 °C. Although this unique structure can provide more reaction sites, it also made the production process more complex and the performance was not competitive. Hence, a cell with this structure needed to be further optimized. Kikuta et al.[91] simplified the preparation process by dip-coating anode slurry on a steel rod substrate with a round end, and then separated the anode support from the steel rod after drying. The final cell produced a peak power density of 0.6 W cm^{-2} at 600 °C. Huang et al.[92] first reported the MT-SOFC fabricated by 3D printing, as shown in Fig. 6d. The anode support was manufactured on the ceramic substrate through 3D printing technology. Compared with the anode manufactured by the extrusion method, the internal NiO and YSZ distribution was more homogeneous dispersion. The final cell with the structure of NiO-YSZ anode, YSZ electrolyte, and proprietary material for cathode, produced a peak power density exceeding 0.989 W cm^{-2} at 800 °C. Ren et al.[93] utilized the phase inversion method to prepare an alumina substrate support, exhibiting the gas permeability nearly ten times higher than that of conventional substrates. The final cell with the structure of NiO-SDC/SDC/PBC exhibited a peak power density of 1.42 W cm^{-2} at 600 °C. The performance of the MT-SOFCs fabricated by different fabrication techniques are summarized in Table 2.

MT-SOFC stacks

MT-SOFC stack development has centered on bundle-based series integration enabled by ceramic manifold and matrix architectures, where optimizing the cathode/matrix material and porosity is crucial to mitigate gas leakage and transport limitations and to retain single-cell-level power density at intermediate temperatures. Suzuki et al.[94] utilized ceramic manifold components to assemble five single cells in series into a stack. The actual images of ceramic manifold components and MT-SOFC stacks consisted of four bundles are shown in Fig. 7a. The maximum output power of the stack with an area of 1.75 cm^2 was 0.4 W at 600 °C. However, due to gas leakage or cell damage, the voltage was only 4 V. Later, Suzuki et al.[95] designed a cathode matrix using LSCF powder for fixing and connecting the MT-SOFCs, which contained three cells to form a bundle. A stack consisting of three bundles was tested and produced a peak power of 1 W with an active area of 5.65 cm^2 at 484 °C. The power density of the stack was lower than that of the single cell, which was probably due to insufficient air supply and gas leakage. Moreover, the design of the LSCF matrix had a significant impact on performance when using the LSCF matrix as the current path. Higher porosity in the LSCF matrix led to decreased conductivity, while lower porosity may result in insufficient oxygen for reactions, thereby affecting performance. Subsequently, Funahashi et al.[96] replaced the cathode matrix material from LSCF to MgO. The schematic diagram of the fabrication process of the stack is showed in Fig. 7b. By using LSCF-Ag conductive paste and MgO insulating paste, the conductive path between the tubular cells was achieved. The peak output power of the three-cell stack exceeded 0.6 W at 500 °C. The peak power density of the stack was 0.22 W cm^{-2}, which was similar to that of a single cell, demonstrating the effectiveness of using MgO cathode matrix to assemble the stack. Such MgO matrix design was later adopted in a model of a 200 W stack was proposed by Funahashi et al.[97].

Zhang et al.[98] utilized metal current collectors and interconnectors to fabricate MT-SOFC stacks. The schematic diagram of the current collector and the assembly process of the eight-cell stack are shown in Fig. 7c. A metallic rod was inserted into the cell with metal brushes in contact with the interior anode surface to collect current. The eight-cell stack provided 17.3 W peak power at 750 °C, which was lower than the expected value due to the high ohmic impedance of the collector and because the actual test temperature was lower than the setting temperature. The temperature gradient between the anode inlet and the fuel leads to high thermal stress. In order to avoid collecting current from the anode inlet, which can cause destruction to the cell, Liang et al.[100] set up a rectangular current collection window in the middle of the anode and used silver pads for electrical connections. Simultaneously, ceramic/glass paste was used for sealing. The final eight-cell stack produced 24.1 W peak output power at 700 °C. To enhance the current collection, the single Ag-pad design was replaced with a double Ni-pad for more efficient current collection, as shown in Fig. 7d[101]. The maximum output power of the 160-cell stack exceeded 1 kW at 700 °C, which was approximately eight times the performance of the 20-cell stack. Therefore, it can be seen that this current collection method was highly effective. Simultaneously, in order to alleviate the high ohmic loss caused by the tubular structure, 3D printing technology was applied to fabricate interconnectors made of

Table 2 The performance of the MT-SOFCs prepared by different fabrication techniques

Fabrication method	Cell composition	Maximum power density (W cm^{-2})	Test temperature (°C)	Ref.
Extrusion	NiO-GDC/GDC/LSCF-GDC	0.857	550	[72]
Extrusion	NiO-GDC/GDC/LSCF-GDC	1.017	550	[74]
Extrusion	NiO-GDC/GDC/LSCF-GDC	1.31	550	[76]
Extrusion	NiO-GDC/GDC/LSCF-GDC	1.31	550	[75]
Phase inversion	NiO-YSZ/YSZ/LSM-YSZ	0.66	850	[87]
Phase inversion	NiO-YSZ/YSZ/LSM-YSZ	0.78	800	[88]
Phase inversion	NiO-YSZ/YSZ/GDC/LSCF-GDC	2.27	700	[22]
Phase inversion	NiO-YSZ/YSZ/LSM-YSZ	0.75	700	[17]
Tape casting combined with isostatic pressing	NiO-YSZ/NiO-YSZ/YSZ/LSM-YSZ	0.293	800	[83]
Dip-coating	NiO/NiO-GDC/GDC/GDC-LSCF	0.6	600	[91]
3D printing	NiO-YSZ/YSZ/Proprietary material	0.989	800	[92]
Phase inversion	Alumina/NiO-SDC/SDC/PBC	1.42	600	[93]

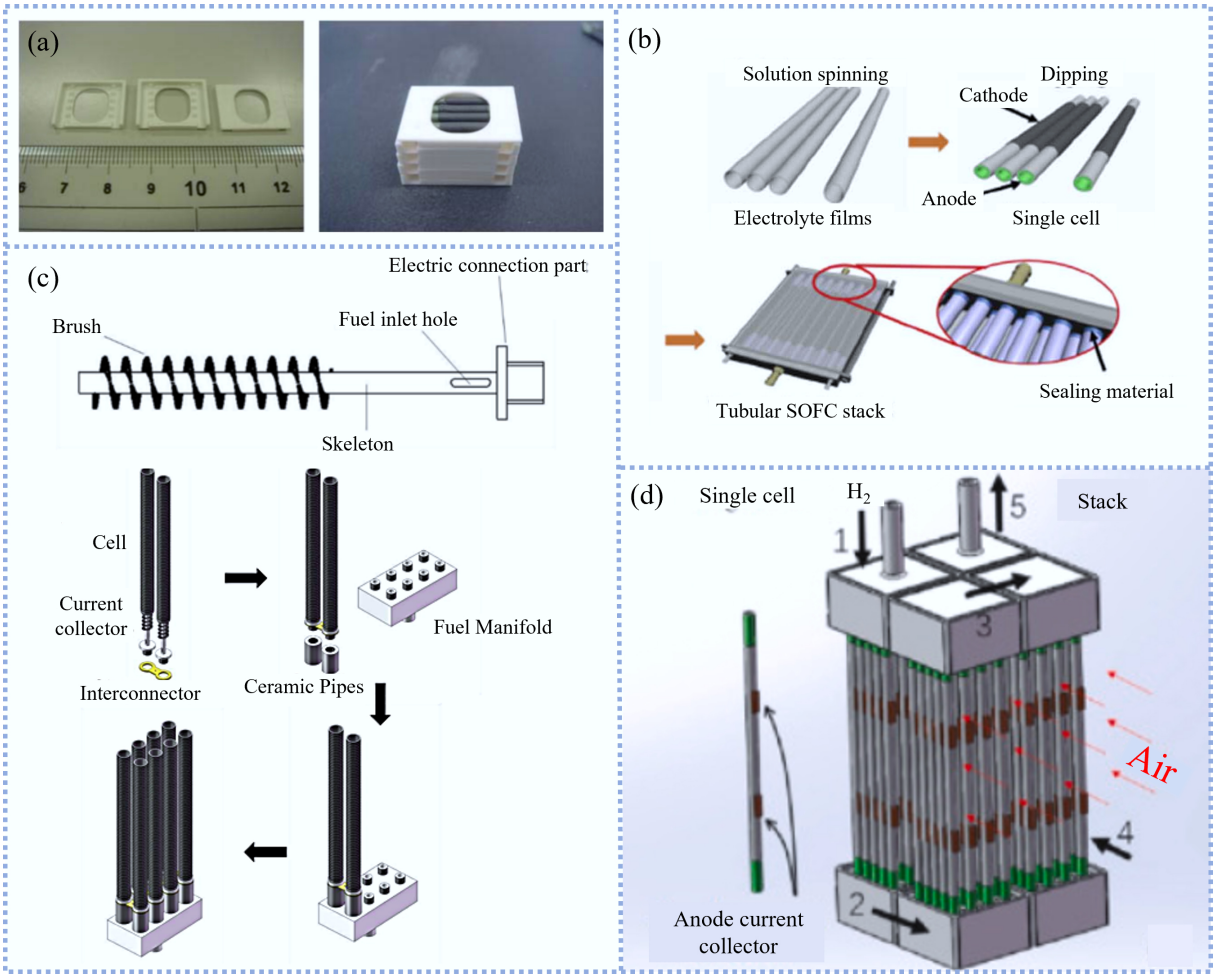

Fig. 7 (**a**) Actual images ceramic manifold components and micro-tubular SOFC stacks consisted of four bundles[94]. (**b**) Fabrication process of the MT-SOFC stack Using MgO matrices[61]. (**c**) Schematic diagram of the current collector and the assembly process of the eight-cell stack[98]. (**d**) Actual images of the MT-SOFC with double Ni-pads and the schematic diagram of the MT-SOFC stack consisting of 80 cells[99].

stainless steel 316[102]. An interconnector was used to connect two single cells in series. To evaluate the interconnector, a single cell was cut into three sections and then connected through the interconnector. The peak power density of the cell was doubled compared to cells with the same axial length.

Tubular SOFCs applications

As an efficient energy conversion technology, SOFCs are gradually receiving widespread attention. In recent years, the progress in cell performance and stability has promoted the application of SOFCs, both as an independent power generation device and as part of an integrated system. As the main type of SOFCs, tubular SOFCs have been widely used in various fields. This chapter introduces the application of tubular SOFCs, and the collected literatures included the type of SOFCs not introduced in the literature.

Tubular SOFCs for transportation

Transportation causes a large amount of carbon dioxide emissions every year. However, decarbonizing transportation is extremely challenging due to the fact that it is difficult to find suitable fuels to replace traditional hydrocarbons. In this background, as technology continues to advance, SOFCs have gained attention as a promising solution. Conventional SOFCs have displayed some major limitations for transportation application such as high working temperatures and slow start-up/shut-down. Additionally, SOFCs feature fragile ceramic components, which pose additional challenges. However, with advancements in materials and cell design, these issues have gradually been mitigated, paving the way for the exploration of SOFCs in various modes of transportation.

A 1 kW SOFC stack on an all-terrain vehicle was installed by Atrex Energy[103], demonstrating stable performance and and only one-third of the fuel consumption of the conventional vehicle during a 3.7 km off-road test loop. Furthermore, no NO_x emissions were detected when CNG was used as the fuel, demonstrating the potential of tubular SOFC in transportation. Jaspers et al.[104] proposed a negative CO_2 emissions method for transportation based on SOFCs electric vehicles. By utilizing carbon-neutral biofuel, the CO_2 produced at the anode was condensed and stored in a pressurized tank for further utilization, thereby achieving carbon-negative emissions. This method significantly reduced the environmental impact of exhaust emissions from SOFC electric vehicles when using hydrocarbon fuels.

In addition, SOFCs can be combined with batteries to supply power for vehicles. The system diagram of SOFCs-battery hybrid vehicle is shown in Fig. 8a. The hybrid system can make up for the

https://doi.org/10.48130/een-0026-0001

soft output characteristics of an SOFCs system alone, allowing the system to respond rapidly to load changes[105]. When the power demand of the vehicle increases rapidly, the battery can supplement the insufficient power of the SOFC system. When the SOFCs system can fulfil the power needs, the excessive electricity can be used to charge the battery.

SOFCs-battery hybrid vehicles were compared with battery electric vehicles, gasoline vehicles, and PEMFCs vehicles based on the situation in Iran[106]. As shown in Fig. 8b, considering fuel prices, capital expenditures, operation and maintenance costs, SOFCs hybrid vehicles were the best choice in the future. However, it was worth noting that this conclusion depended on Iran's abundant natural gas resources and related infrastructure. Bessekon et al.[108] established and verified a model of SOFCs-battery electric vehicles. A 12 kW SOFCs system was integrated into a model of the electric vehicle. The range was significantly increased when using CNG, LNG, or LPG as fuel. Especially, the energy consumption was much lower than that of internal combustion engine vehicles. Therefore, it can be concluded that integrating SOFC with vehicles is highly competitive.

Due to the various advantages of SOFCs, researchers integrated an SOFCs system into the unmanned aerial vehicle (UAV) to develop more advanced power systems, which can significantly increase flight duration compared to battery electric UAVs. Adelan Ltd and the University of Birmingham[107] successfully developed a UAV, the Skywalker X8 UAV, powered by an MT-SOFCs stack and battery as shown in Fig. 8c, d, respectively. The UAV had a wingspan of 2 m and a total weight of 6 kg, of which the MT-SOFC system weighed 2.5 kg. The anode manifold was fabricated by 3D printing technology, which greatly reduced the weight of the MT-SOFCs stack. The SOFC system used liquid propane as fuel, and the catalytic partial oxidation catalyst was positioned inside the MT-SOFCs, which can improve the gravimetric power density of the system but diminish the system efficiency. Finally, the gravimetric power density of the MT-SOFC stack system was 100 W kg^{-1}. Notably, the power required during the takeoff phase of the aircraft was relatively high, which was provided by the SOFCs stack and battery. During cruise or landing, the SOFCs system supplied power, while recharging the battery simultaneously. Ultra Electronics USSI received a $1.2 million contract to develop UAV systems powered by D245XR and D350XR

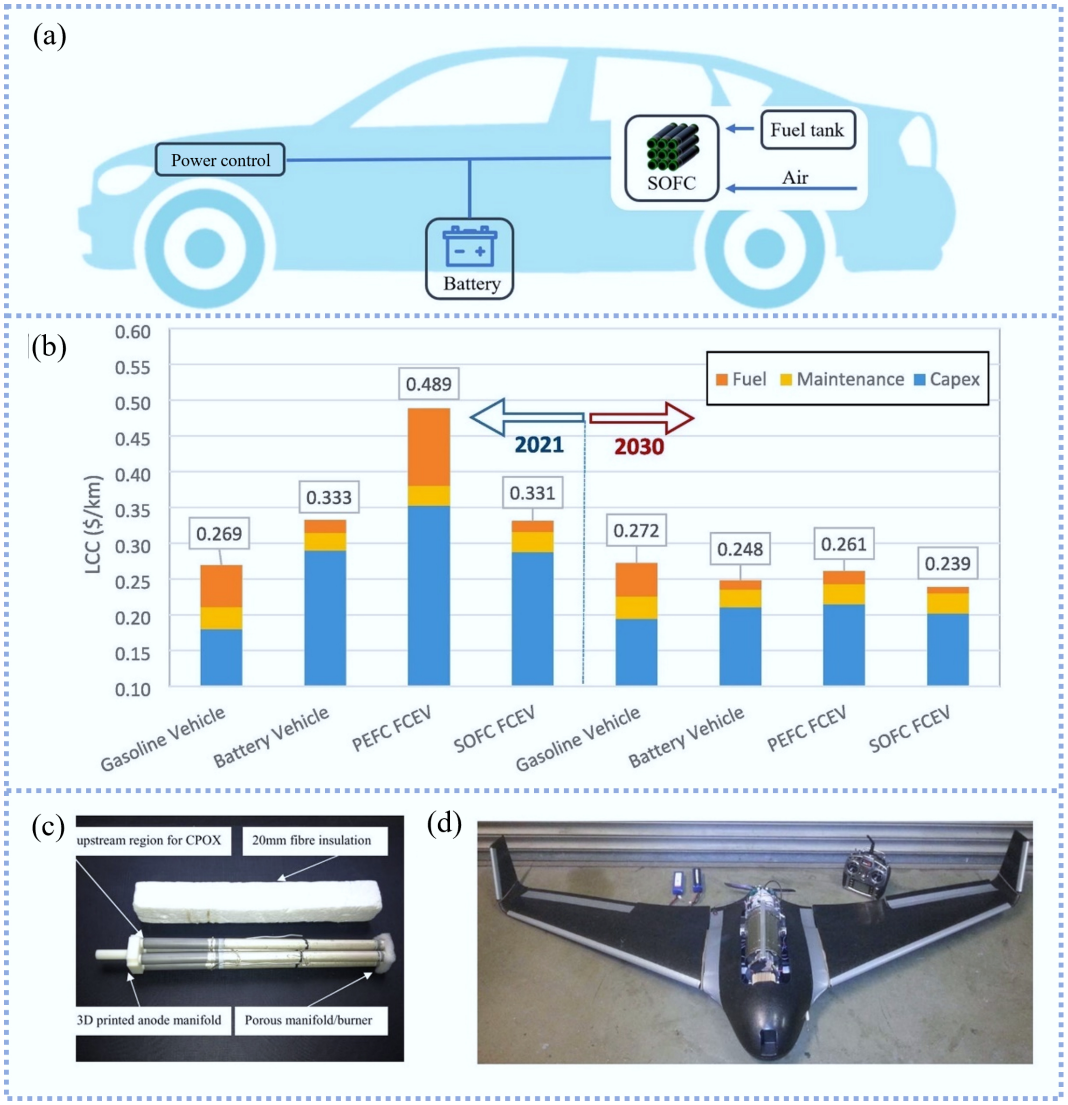

Fig. 8 (**a**) System diagram of SOFCs-battery hybrid vehicle. (**b**) Life cycle costs of different vehicles[106]. (**c**) MT-SOFCs stack for the UAV. (**d**) Actual images of UAV equipped with MT-SOFC system[107].

SOFC[109]. The SOFCs power system allowed UAV to increase flight duration and can carry more sensors to perform different tasks. By using propane as fuel, the energy density of the SOFCs system was ten times higher than that of a battery. It can be concluded that SOFC powered UAVs have significant potential and application prospects. However, further research is imperative to guarantee the stable running of the entire system. Bahari et al.[110] compared SOFCs power systems using hydrogen and methane as fuel, respectively. The influences of various conditions such as flight altitude, the design and working conditions of SOFCs power system on UAV were investigated. The results showed that the output power and efficiency of the SOFCs system increased with the flight altitude when using methane as the fuel, while hydrogen-fueled systems showed greater competitiveness in low-altitude flights due to the fact that the efficiency and power increased with the decrease of the flight altitude. Increasing the fuel rate of the SOFCs system can improve the output power, but excessive fuel supplied will decrease the efficiency of the power system and result in a decrease in flight duration. To prevent the malfunction of the SOFCs system in the UAV, causing excessive local temperature inside the UAV. Therefore, there must be proper ventilation around the SOFCs power system. Giacoppo et al.[111] established a CFD model to investigate airflow distribution and temperature distribution inside the UAV. The results indicated the necessity of proper insulation for the fuselage and exhaust interface of the SOFC generator body to prevent overheating of the pod shell, which can affect the normal operation of the drone.

Tubular SOFCs-based CHP system for residence

SOFCs are featured by high working temperatures and low noise due to the absence of mechanical components and the ability of supplying power and high-grade exhaust gas simultaneously[112]; they are an ideal option to assemble SOFCs into the CHP systems to utilize waste heat for residential and industrial applications. Figure 9a is the general layout of a typical SOFCs-based CHP system. The power generated by the SOFCs fulfils the requirement of the residence, whereas the excess power could be transported to the grid. When the system cannot fulfil the power needs of the residence, electricity can be purchased from the grid. The waste heat produced by SOFCs is utilized to heat water and supply heat to the residence, as shown in Fig. 9b.

The 100 kW SOFCs-based CHP system developed by Siemens Westinghouse was delivered to EDB/ELSAM (a Dutch/Danish utility consortium) at the end of 1997[115]. The SOFC stack consists of 24 modules containing 1,152 cells and each single cell had an active area of 834 cm^2[115]. The SOFCs-based CHP system operated on natural gas as the fuel, delivering 105 to 110 kW of net AC power to the grid and about 65 kW of net AC power to the heating system. An electrical efficiency (net AC/LHV) of 46% was achieved during the spring and summer of 1999.

In 2004, a 1 kW SOFC-based CHP system was developed and installed in a residential setting for demonstration[116]. The SOFCs module consisted of SOFCs stack, heat exchange components and a reforming reactor[117]. During operation, the output power of the SOFCs stack can be automatically adjusted according to the requirements of the residence. Operating at rated power, the electrical efficiency of the system was 49% (net ac, LHV), exceeding the average grid efficiency of Japanese power plants based on fossil fuel. Subsequently, Kyocera, Osaka Gas, Toyota Motor and Aisin Seiki collaborated to develop a new SOFCs-based CHP system. In order to be better suited for in-house installation, the size of the system was significantly reduced by adopting a flat-tubular design, while the rated power of the system was reduced from 1 kW to 700 W. In 2012, the commercialized SOFCs-based CHP system 'Ene Farm type S' was launched, as shown in Fig. 9c[113]. However, the electrical efficiency of the system was 46.5% (LHV). After upgrading, such as improving the air flow in the stack and improving the control accuracy of gas flow, Ene Farm type S (2016 model) exhibited an enhanced electrical efficiency of 52% (LHV)[118].

On the other hand, numerous simulations on the application of SOFCs-based CHP systems in buildings have been conducted recently. Wakui et al.[119] investigated the operation strategy of the SOFCs-based CHP in residential areas. It was stipulated that the power generated by SOFCs can be shared among households within residential areas to form a micro-grid. However, the power produced by SOFC was not allowed to be delivered to commercial power systems. The schematic diagram of micro-grid composed of SOFCs-based CHP in residential area is shown in Fig. 9d. Then, two control strategies of the SOFCs-based CHP system were compared, namely prioritizing power demand and hot water demand, respectively. Based on the data from 20 households, it was concluded that strategy one can improve the electrical load factor of the system and have a high energy-saving effect. Meanwhile, maintaining the high efficiency of power generation in SOFCs-based CHP system was crucial for the competitiveness of the system during power exchange. Pirkandi et al.[120] investigated the effect of working conditions on the SOFCs-based CHP system through simulation. The results showed that raising the working temperature of the SOFCs was beneficial to the electrical efficiency of the system but the thermal efficiency was reduced. Increasing the working pressure had the opposite effect but both strategies can improve overall system efficiency. It was also concluded that when residence units required high electrical loads and low thermal loads, SOFCs with higher operating temperatures should be given priority. Baniasadi & Alemrajabi[121] established a model of a 215 kW SOFCs stack combined with a recovery cycle to fulfil the living needs of a hotel with an area of 4,600 m^2, while the energy and exergy analyses of the individual components were conducted. The results showed that the system can achieve a peak efficiency of 83% for simultaneous power generation and heat recovery cycles. Moreover, the system can fulfil all power and cooling load as well as 40% of the hot water demand. In the latest studies, Narayanan et al.[122] simulated the integration of SOFCs-based CHP systems using natural gas as fuel and other energy systems to fulfil the energy needs of residential buildings. The results showed that achieving 100% self-supply of the electrical loads through SOFCs-based CHP was possible. Yang et al.[123] investigated the operation of SOFCs and micro-CHP systems in residential applications in five distinct climate zones in China. The results showed that it was difficult to meet the thermal demand of residences in cold areas with the SOFCs-CHP system, necessitating the use of auxiliary equipment. Fong et al.[124] used numerical simulation to evaluate a 2 kW SOFCs-based CHP system for a residential building in Hong Kong (China), showing a reduction in primary energy utilization and carbon dioxide emissions compared to traditional systems. In general, SOFCs-based CHP system exhibited high energy efficiency and was environmentally friendly. However, in some cold areas, it is a challenge for the small-scale SOFCs-based CHP system alone to meet the power and heat demand.

Tubular SOFCs integrated with gas turbines

In addition to CHP system, the high-grade waste heat could be adopted by gas turbines (GT), which improves the overall energy utilization of the system. According to different working pressures,

https://doi.org/10.48130/een-0026-0001

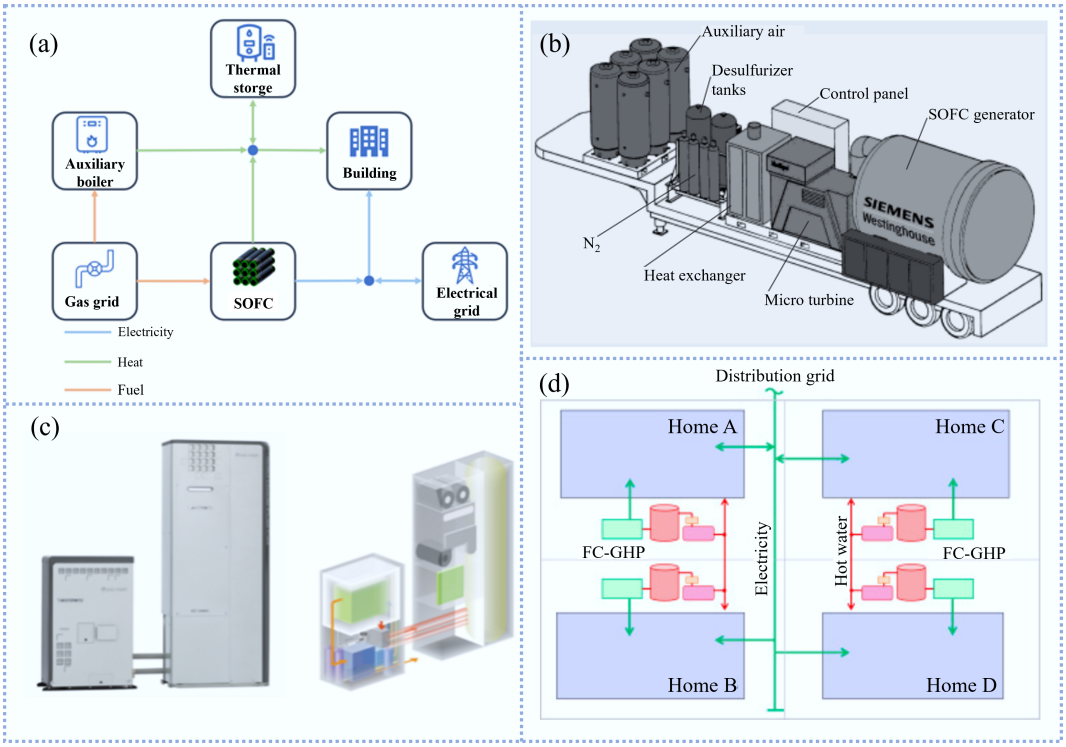

Fig. 9 (**a**) General layout of a typical SOFCs-based CHP system. (**b**) SOFCs-based CHP system developed by Siemens Westinghouse[19]. (**c**) Commercial SOFCs-based CHP system 'Ene Farm type S'[113]. (**d**) Schematic diagram of micro-grid composed of SOFCs-based CHP system in residential area[114].

SOFCs-GT systems are mainly divided into ambient pressure systems and pressurized systems. The SOFCs-GT system exhibits high reliability and stabilizes the turbine inlet gas temperature when operating under ambient pressure. Nevertheless, operating under pressurized conditions allows for higher efficiency[125]. Park & Kim[126] established a model to compare the performance of two types of SOFCs-GT systems. The results indicated that the pressurized SOFCs-GT system exhibited superior efficiency, while the efficiency of ambient pressure hybrid systems with a high pressures ratio may be lower than that of the SOFCs only system. Therefore, the pressurized SOFCs-GT system is used in most cases.

Figure 10a is the schematic diagram of a pressurized SOFCs-GT system. The air is compressed to the working pressure of the SOFCs and then heated by a heat exchanger. The pre-heated air enters the SOFCs stack, where it reacts electrochemically with the compressed fuel to produce electricity. The cathode exhaust gas and remaining fuel are completely burned in the combustor and then enter the turbine. The airflow expands inside the turbine, driving the generator to produce electricity. The exhaust gas from the GT is delivered to the heat exchanger, thereby improving energy efficiency.

In 1997, SCE signed a contract with Westinghouse Electric to manufacture a SOFCs-GT system[115]. A 220 kWe power system based on tubular SOFCs stack consisted of 1,152 cells, with a cell diameter of 22 mm and a length of 1,500 mm, connected in series/parallel. In addition to the SOFCs module, the SOFCs-GT system also included four main modules: fuel supply, electrical and power dissipation devices, thermal management (including micro-turbine generator) and heat export. The system without the power dissipator is shown in Fig. 10b. With natural gas as the fuel, SOFCs module operated at pressurized condition of 3 atm. During initial testing, the total power of SOFCs and MGT DC was 166 and 22 kW, respectively[126].

Mitsubishi Heavy Industries (MHI) manufactured and tested a 200 kW SOFCs-MGT system based on the SIS-SOFC stack and the SOFC module is shown in Fig. 10c[127]. The system achieved the peak power of 229 kW-AC and the peak efficiency of 52.1% LHV. The system remained stable for 3,224 h. Subsequently, Mitsubishi Hitachi Power Systems (MHPS) further manufactured a 250 kW SOFCs-MGT system, as shown in Fig. 10d, and conducted various practicability evaluation tests to test system performance[66]. The results indicated that the electrical output power of the system was approximately 204 kW and the power generation efficiency reached 53.6% LHV during rated-output operation. During the 25,000 h of rated-output operation, the SOFCs stack remained stable after repeated start-up/shut-down. Moreover, the system exhibited the ability to efficiently recover waste heat with a total efficiency of 74.1% LHV, so it had excellent potential for energy saving and emission reduction[129].

In addition, numerous theoretical studies on the SOFCs-GT systems have been reported. Zhang et al.[130] conducted research on the rapid load switching of the SOFCs-GT system to ensure stability of the grid when renewable energy was integrated. Bypass valves were set up to regulate the flow of SOFCs cathode gas during load switching, while the fuel utilization was sustained by changing the fuel flow. The pre-combustion and after-combustion chambers were set up to balance heat requirements. With these control strategies, a 50% load change can be achieved in just 10 s while protecting the SOFC stack. Lai et al.[131] conducted a cradle-to-product life cycle study of four types of SOFCs power plants to understand the life cycle environmental impacts of the SOFCs applications in the systems. The results indicated that the SOFCs-GT hybrid plant with steam cycle was considered the optimal alternative, while it was also concluded that operating the SOFCs stack in constant voltage mode will extend the service life of the SOFCs stack compared to constant

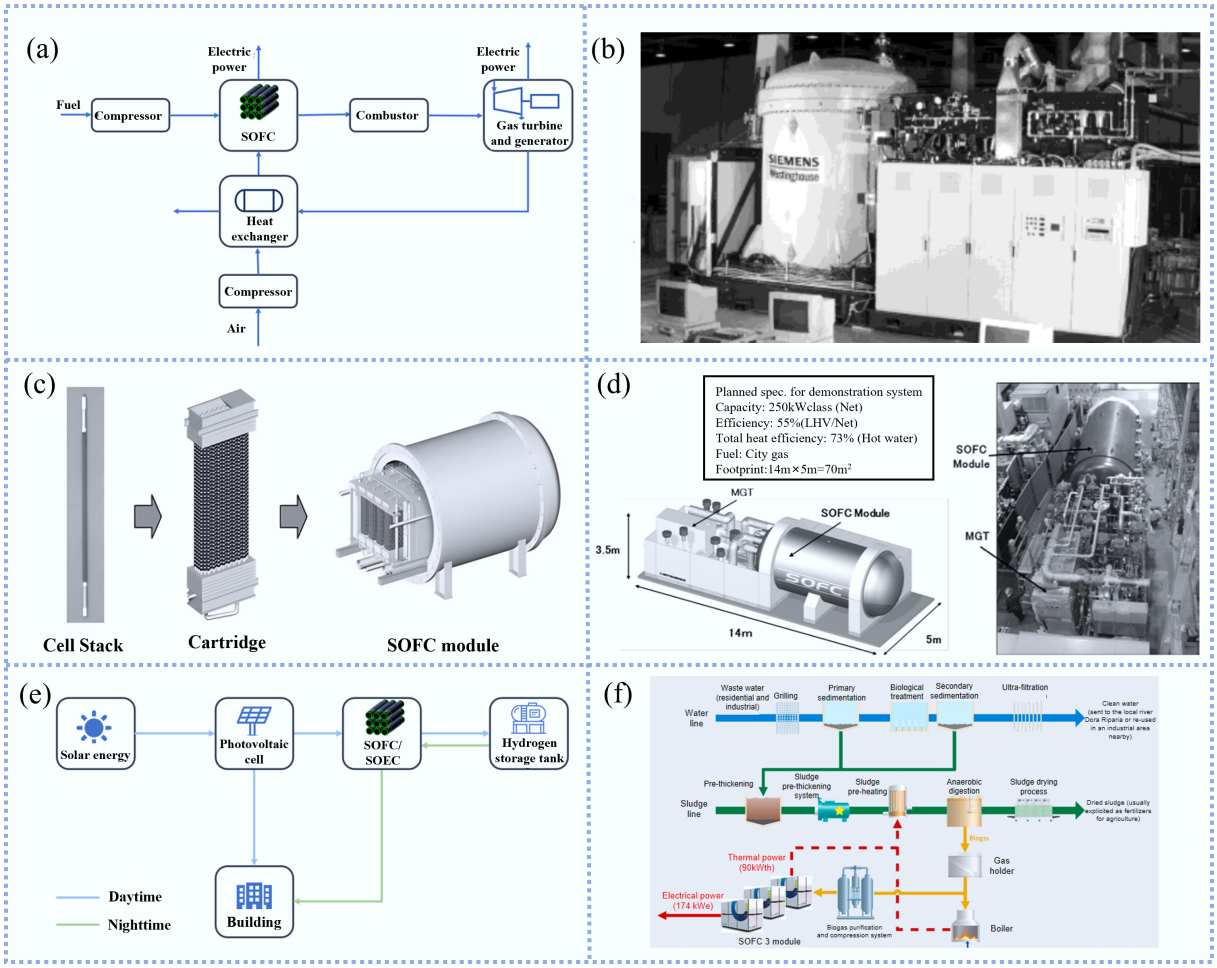

Fig. 10 (**a**) Schematic diagram of a pressurized SOFCs-GT system. (**b**) 220 kW SOFCs-GT system without the power dissipators[19]. (**c**) SOFC module developed by MHI[127]. (**d**) 250 kW SOFCs-GT system was developed by MHPS[66]. (**e**) Schematic diagram of a system combining SOFCs and photovoltaics. (**f**) Layout of wastewater treatment plant with SOFCs[128].

power operation. van Biert et al.[132] analyzed four SOFCs combined cycles and showed that pressurized SOFCs-GT systems exhibited higher electrical efficiency at high temperature and moderate cell voltage. On the other hand, the SOFCs-steam turbine combined cycle was more competitive at low temperature and high cell voltage. Sghaier et al.[133] established a thermodynamic and electrochemical model containing SOFCs-GT, conducted a parameter study on SOFCs-GT, and pointed out that an increase in ambient humidity and temperature will reduce the efficiency of the power plant.

Tubular SOFCs integrated with renewable energy

As typical types of renewable energy, solar power and wind power suffer from intermittency issues, which necessitate their integration with other technologies for uninterrupted power supply. SOFCs/SOECs have gained attention as a promising solution due to their flexible reversibility. By optimizing the system design, SOFCs exhibit excellent load-reactive capabilities[134]. Moreover, SOFCs can maintain high-efficiency under partial load, which is relatively difficult with gas turbine[135]. Figure 10e depicts the schematic diagram of a system combining SOFCs and photovoltaics. During the day time, solar energy is converted into electricity through photovoltaic cells, with excessive power used to produce hydrogen through the SOECs while meeting the electricity demand. When solar radiation is insufficient, a stable power supply is ensured through the SOFCs system. In this way, the hybrid system based on photovoltaic power generation system and SOFC achieves all-weather power supply.

Xi et al.[136] integrated solar chimneys and SOFCs into a system, the electricity was generated through solar chimney operation during the day time, and excessive power was used to produce hydrogen through the SOECs. When solar radiation was insufficient, the solar chimney cannot fulfil the power demand and the SOFCs started to generate electricity. The integrated system made up for the limitation that the solar chimney cannot work at night, achieving long-term continuous power supply. Shariatzadeh et al.[137] utilized the same strategy to compensate for the shortcomings of photovoltaic systems that cannot continue to work.

Apart from generating electricity through photovoltaic cells, solar energy can be used to fulfil thermal demand. Gandiglio et al.[128] coupled SOFCs with a wastewater treatment plant, and the plant floor plan is shown in Fig. 10f. The biogas generated by the anaerobic digester was converted into fuel through the reformer and then entered the SOFCs stack for power generation. The heat discharged from the SOFCs stack was recovered to fulfil partial heat demand of the anaerobic digester, while the concentrated solar thermal system also supplied heat to the digester. In the life cycle impact assessment (LCIA), the biogas-fed SOFC cogeneration modules reduce the environmental burden associated to WWTPs with a substantial share

https://doi.org/10.48130/een-0026-0001

of electrical energy (around 25%) production. Azadi[138] established a system model to produce methane and hydrogen utilizing solar collectors coupled with the catalytic hydrothermal glycerol reforming. The heat required in the process of the catalytic hydrothermal reforming of glycerol was provided by the solar collector. After removing water, the generated gas can be used as fuel for SOFCs. Moreover, when using other oxygenated biomass compounds, only minor change to the system were required. In addition, there are research works on SOFCs integrated with wind power system[139–141], and microgrids composed of SOFCs and renewable energy[142,143].

In general, the system coupling SOFCs and renewable energy dramatically extends the range of SOFC application. Meanwhile, the integrated system effectively addresses the long-existing intermittency issue of renewable energy, which enables stable and continuous operation.

Conclusion and future perspectives

In conclusion, tubular SOFCs technology offers distinct advantages and significant prospects compared to traditional fossil fuel-based power generation. This review has systematically introduced the manufacturing processes, stack assembly designs, and application status of tubular SOFCs. The main conclusions are summarized as follows:

1. Geometric optimization: Each geometric configuration possesses unique advantages suitable for specific applications. FT-SOFCs offer higher volumetric power density, making FT-SOFCs advantageous for stationary power generation (kilowatt level), though sealing remains a key limitation. Both SIS-SOFCs and cone-shaped SOFCs achieve higher voltages in limited spaces but face challenges in interconnection integrity. To date, while the FT and SIS stacks have reached the kilowatt level, scaling to the megawatt level requires overcoming these structural hurdles. Conversely, MT-SOFCs, with their high specific surface area and rapid start-up capabilities (exceeding 2 W cm^{-2}), are ideal for portable and UAV power systems. A major challenge for MT-SOFCs lies in optimizing current collection for kilowatt-class scaling.

2. Fabrication advances: The fabrication process critically determines cell performance. While extrusion method and phase inversion are the mainstream methods allowing for single-step multi-layer preparation, phase inversion offers superior control over the internal pore structure of the support. Future development should focus on refining these processes to reduce sintering costs and enhance mass transport properties.

3. Integration and waste heat utilization: Tubular SOFCs can be used as independent power units due to their mechanical robustness and thermal shock resistance. Additionally, their high grades waste heat offers significant opportunities for integration with other systems (e.g., CHP or gas turbine), which is essential for improving overall system efficiency and economic viability.

4. Future perspectives: Reversible operation and hydrogen production: In future development, the utilization of SOFCs waste heat will become a key research focus to further enhance the energy efficiency and economy of the system. The operation of tubular cells in reversible mode (r-SOC) for green hydrogen production and energy storage is a critical research frontier. Tubular designs are intrinsically well-suited for r-SOC applications due to their high mechanical strength, which can withstand the high pressures required for efficient electrolysis, and their simplified sealing which mitigates gas leakage risks. However, several specific technical challenges remain:

Electrode stability: Long-term degradation of the air electrode under high steam concentrations (in electrolysis mode) needs to be addressed through novel material design.

Thermal management: Efficient thermal management strategies must be developed to handle the transition between exothermic (fuel cell) and endothermic (electrolysis) modes to prevent thermal stress accumulation.

System response: Improving the dynamic response rate of the stack to couple effectively with intermittent renewable energy sources (solar/wind) is crucial for achieving grid-level energy storage and carbon neutrality.

Author contributions

The authors confirm their contributions to the paper as follows: Tong Wang: conceptualization, writing – original draft, writing – review & editing; Yanling Feng: visualization, revising – original draft; Yeqing Ling: visualization, resources; Bin Wang: investigation, methodology; Yakun Wang: conceptualization, resources; Mohd Hafiz Dzarfan Othman: investigation, methodology; Tao Li: conceptualization, funding acquisition, project administration, resources, writing – review & editing. All authors reviewed the results and approved the final version of the manuscript.

Data availability

Data sharing is not applicable to this article as no datasets were generated or analyzed during the current study.

Funding

This research was funded by the National Natural Science Foundation of China (Grant Nos U24A20542, 52276175), and the Natural Science Foundation of Jiangsu Province (Grant No. BK20210252).

Declarations

Competing interests

The authors declare that there is no conflict of interest.

Author details

[1]MOE Key Laboratory of Energy Thermal Conversion & Control, School of Energy and Environment, Southeast University, Nanjing 210096, China; [2]School of Electrical Engineering, Tongling University, Tongling 244061, China; [3]Advanced Membrane Technology Research Centre (AMTEC), Faculty of Chemical and Energy Engineering, Universiti Teknologi Malaysia (UTM), Skudai, Johor Bahru 81310, Malaysia

References

[1] He W, Zou J, Wang B, Vilayurganapathy S, Zhou M, et al. 2013. Gas transport in porous electrodes of solid oxide fuel cells: a review on diffusion and diffusivity measurement. *Journal of Power Sources* 237:64–73

[2] Choudhary T, Sanjay. 2017. Thermodynamic assessment of SOFC-ICGT hybrid cycle: energy analysis and entropy generation minimization. *Energy* 134:1013–1028

[3] Hassan N. 2021. Catalytic performance of nanostructured materials recently used for developing fuel cells' electrodes. *International Journal of Hydrogen Energy* 46:39315–39368

[4] Singhal SC. 2000. Advances in solid oxide fuel cell technology. *Solid State Ionics* 135:305–313

[5] Chehrmonavari H, Kakaee A, Hosseini SE, Desideri U, Tsatsaronis G, et al. 2023. Hybridizing solid oxide fuel cells with internal combustion engines for power and propulsion systems: a review. *Renewable and Sustainable Energy Reviews* 171:112982

[6] Suzuki T, Liang B, Yamaguchi T, Hamamoto K, Fujishiro Y. 2011. Development of novel micro flat-tube solid-oxide fuel cells. *Electrochemistry Communications* 13:719–722

[7] Kong W, Zhang W, Zhang S, Zhang Q, Su S. 2016. Residual stress analysis of a micro-tubular solid oxide fuel cell. *International Journal of Hydrogen Energy* 41:16173–16180

[8] Li T, Heenan TMM, Rabuni MF, Wang B, Farandos NM, et al. 2019. Design of next-generation ceramic fuel cells and real-time characterization with synchrotron X-ray diffraction computed tomography. *Nature Communications* 10:1497

[9] Leah RT, Bone A, Hammer E, Selcuk A, Rahman M, et al. 2017. Development progress on the ceres power steel cell technology platform: further progress towards commercialization. *ECS Transactions* 78:87

[10] Mukerjee S, Leah R, Selby M, Stevenson G, Brandon NP. 2017. Chapter 9 - Life and reliability of solid oxide fuel cell-based products: a review. In *Solid Oxide Fuel Cell Lifetime and Reliability*, eds. Brandon NP, Ruiz-Trejo E, Boldrin. UK: Academic Press. pp. 173–191 doi: 10.1016/B978-0-08-101102-7.00009-X

[11] Mai A, Schuler JA, Fleischhauer F, Nerlich V, Schuler A. 2015. Hexis and the SOFC system Galileo 1000 N: experiences from lab and field testing. *ECS Transactions* 68:109

[12] Mai A, Iwanschitz B, Schuler JA, Denzler R, Nerlich V, et al. 2013. Hexis' SOFC system Galileo 1000 N – lab and field test experiences. *ECS Transactions* 57:73

[13] Cable TL, Sofie SW. 2007. A symmetrical, planar SOFC design for NASA's high specific power density requirements. *Journal of Power Sources* 174:221–227

[14] Singhal SC. 2014. Solid oxide fuel cells for power generation. *WIREs Energy and Environment* 3:179–194

[15] Han Z, Wang Y, Yang Z, Han M. 2016. Electrochemical properties of tubular SOFC based on a porous ceramic support fabricated by phase-inversion method. *Journal of Materials Science & Technology* 32:681–686

[16] Kuterbekov KA, Nikonov AV, Bekmyrza KZ, Pavzderin NB, Kabyshev AM, et al. 2022. Classification of solid oxide fuel cells. *Nanomaterials* 12:1059

[17] Ab Rahman M, Othman MHD, Fansuri H, Harun Z, Omar AF, et al. 2020. Development of high-performance anode/electrolyte/cathode micro-tubular solid oxide fuel cell via phase inversion-based co-extrusion/co-sintering technique. *Journal of Power Sources* 467:228345

[18] Howe KS, Thompson GJ, Kendall K. 2011. Micro-tubular solid oxide fuel cells and stacks. *Journal of Power Sources* 196:1677–1686

[19] Hassmann K. 2001. SOFC power plants, the Siemens-Westinghouse approach. *Fuel Cells* 1:78–84

[20] Dollard WJ. 1992. Solid oxide fuel cell developments at Westinghouse. *Journal of Power Sources* 37:133–139

[21] Othman MHD, Wu Z, Droushiotis N, Doraswami U, Kelsall G, et al. 2010. Single-step fabrication and characterisations of electrolyte/anode dual-layer hollow fibres for micro-tubular solid oxide fuel cells. *Journal of Membrane Science* 351:196–204

[22] Li T, Lu X, Rabuni MF, Wang B, Farandos NM, et al. 2020. High-performance fuel cell designed for coking-resistance and efficient conversion of waste methane to electrical energy. *Energy & Environmental Science* 13:1879–1887

[23] Kendall K, Minh NQ, Singhal SC. 2003. Chapter 8 – Cell and stack designs. In *High Temperature and Solid Oxide Fuel Cells: Fundamentals, Design and Applications*, eds. Singhal SC, Kendall K. Amsterdam: Elsevier. pp. 197–228 doi: 10.1016/B978-185617387-2/50025-8

[24] Singhal SC. 2000. Science and technology of solid-oxide fuel cells. *MRS Bulletin* 25:16–21

[25] Behling NH. 2013. Chapter 6 - History of solid oxide fuel cells. In *Fuel Cells*, ed. Behling NH. Amsterdam: Elsevier. pp. 223–421 doi: 10.1016/B978-0-444-56325-5.00006-5

[26] Kendall K. 2010. Progress in microtubular solid oxide fuel cells. *International Journal of Applied Ceramic Technology* 7:1–9

[27] Sui J, Liu J. 2007. An electrolyte-supported SOFC stack fabricated by slip casting technique. *ECS Transactions* 7:633

[28] Timurkutluk B, Timurkutluk C, Mat MD, Kaplan Y. 2016. A review on cell/stack designs for high performance solid oxide fuel cells. *Renewable and Sustainable Energy Reviews* 56:1101–1121

[29] Khan MZ, Iltaf A, Ishfaq HA, Khan FN, Tanveer WH, et al. 2021. Flat-tubular solid oxide fuel cells and stacks: a review. *Journal of Asian Ceramic Societies* 9:745–770

[30] Lim TH, Park JL, Lee SB, Park SJ, Song RH, et al. 2010. Fabrication and operation of a 1 kW class anode-supported flat tubular SOFC stack. *International Journal of Hydrogen Energy* 35:9687–9692

[31] Kim SD, Hyun SH, Moon J, Kim JH, Song RH. 2005. Fabrication and characterization of anode-supported electrolyte thin films for intermediate temperature solid oxide fuel cells. *Journal of Power Sources* 139:67–72

[32] Park S, Sammes NM, Song KH, Kim T, Chung JS. 2017. Monolithic flat tubular types of solid oxide fuel cells with integrated electrode and gas channels. *International Journal of Hydrogen Energy* 42:1154–1160

[33] Wang J, Zhao Y, Yang J, Sang J, Wu A, et al. 2023. Understanding thermal and redox cycling behaviors of flat-tube solid oxide fuel cells. *International Journal of Hydrogen Energy* 48:21886–21897

[34] Yoon H, Kim T, Park S, Sammes NM, Chung JS. 2018. Stable LSM/LSTM bi-layer interconnect for flat-tubular solid oxide fuel cells. *International Journal of Hydrogen Energy* 43:363–372

[35] Liu W, Zou Z, Miao F, Li X, Wang J, et al. 2019. Anode-Supported Planar Solid Oxide Fuel Cells Based on Double-sided Cathodes. *Energy Technology* 7:240–244

[36] Liu W, Zheng J, Wang Y, Jiang C, Li D, et al. 2020. Structure evaluation of anode-supported planar solid oxide fuel cells based on single/double-sided electrolyte(s) under redox conditions. *International Journal of Applied Ceramic Technology* 17:1314–1321

[37] Guan W, Du Z, Wang J, Jiang L, Yang J, et al. 2020. Mechanisms of performance degradation induced by thermal cycling in solid oxide fuel cell stacks with flat-tube anode-supported cells based on double-sided cathodes. *International Journal of Hydrogen Energy* 45:19840–19846

[38] Yang J, Zou Z, Zhang H, Chang X, Liu W, et al. 2021. Study on the long-term discharge and redox stability of symmetric flat-tube solid oxide fuel cells. *International Journal of Hydrogen Energy* 46:9741–9748

[39] Khan MZ, Song RH, Hussain A, Lee SB, Lim TH, et al. 2020. Effect of applied current density on the degradation behavior of anode-supported flat-tubular solid oxide fuel cells. *Journal of the European Ceramic Society* 40:1407–1417

[40] Lim TH, Kim GY, Park JL, Song RH, Lee SB, et al. 2007. Operating characteristics of advanced 500W class anode-supported flat tubular SOFC stack in KIER. *ECS Transactions* 7:193

[41] Ji W, Zhang L, Ming L, Jiang Y, Xie B. 2015. Design and fabrication of a 600W anode supported flat tubular SOFC stack. *ECS Transactions* 68:1865

[42] Choi Y, Byun S, Seo DW, Hwang HJ, Kim TW, et al. 2022. New design and performance evaluation of 1 kW-class reversible solid oxide electrolysis-fuel cell stack using flat-tubular cells. *Journal of Power Sources* 542:231744

[43] Han B, Tang Y, Wang J, Guan W, Singhal SC. 2023. Degradation behavior under alternating constant-current/constant-voltage discharge for flat-tube solid oxide fuel cells inside stack. *International Journal of Hydrogen Energy* 48:17654–17663

[44] Sui J, Liu J. 2008. Slip-cast $Ce_{0.8}Sm_{0.2}O_{1.9}$ cone-shaped SOFC. *Journal of the American Ceramic Society* 91:1335–1337

[45] Sui J, Dong L, Liu J. 2012. Cone-shaped cylindrical $Ce_{0.9}Gd_{0.1}O_{1.95}$ electrolyte prepared by slip casting and its application to solid oxide fuel cells. *Journal of Rare Earths* 30:53–56

[46] Zhang Y, Liu J, Yin J, Yuan W, Sui J. 2008. Fabrication and performance of cone-shaped segmented-in-series solid oxide fuel cells. *International Journal of Applied Ceramic Technology* 5:568–573

[47] Bai Y, Liu J, Wang C. 2009. Performance of cone-shaped tubular anode-supported segmented-in-series solid oxide fuel cell stack fabricated by dip coating technique. *International Journal of Hydrogen Energy* 34:7311–7315
[48] Ding J, Liu J. 2009. A novel design and performance of cone-shaped tubular anode-supported segmented-in-series solid oxide fuel cell stack. *Journal of Power Sources* 193:769–773
[49] Ding J, Liu J. 2008. Fabrication and Electrochemical Performance of Anode-Supported Solid Oxide Fuel Cells by a Single-Step Cosintering Process. *Journal of the American Ceramic Society* 91:3303–3307
[50] Liu Y, Tang Y, Ding J, Liu J. 2012. Electrochemical performance of cone-shaped anode-supported segmented-in-series SOFCs fabricated by gel-casting technique. *International Journal of Hydrogen Energy* 37:921–925
[51] Xiao J, Liu J, Ding J. 2011. Electrochemical performance of cone-shaped tubular anode supported solid oxide fuel cells fabricated by low-pressure injection moulding technique. *ECS Transactions* 35:609
[52] Wang H, Liu J. 2012. Effect of anode structure on performance of cone-shaped solid oxide fuel cells fabricated by phase inversion. *International Journal of Hydrogen Energy* 37:4339–4345
[53] Zhang SL, Li CX, Liu S, Li CJ, Yang GJ, et al. 2017. Thermally sprayed large tubular solid oxide fuel cells and its stack: geometry optimization, preparation, and performance. *Journal of Thermal Spray Technology* 26:441–455
[54] Gardner FJ, Day MJ, Brandon NP, Pashley MN, Cassidy M. 2000. SOFC technology development at Rolls-Royce. *Journal of Power Sources* 86:122–129
[55] Yoshida H, Seyama T, Sobue T, Yamashita S. 2011. Development of residential SOFC CHP system with flatten tubular segmented-in-series cells stack. *ECS Transactions* 35:97
[56] Park BK, Kim DW, Song RH, Lee SB, Lim TH, et al. 2015. Design of a dual-layer ceramic interconnect based on perovskite oxides for segmented-in-series solid oxide fuel cells. *Journal of Power Sources* 300:318–324
[57] Mushtaq U, Kim DW, Yun UJ, Lee JW, Lee SB, et al. 2015. Effect of cathode geometry on the electrochemical performance of flat tubular segmented-in-series (SIS) solid oxide fuel cell. *International Journal of Hydrogen Energy* 40:6207–6215
[58] Kim DW, Yun UJ, Lee JW, Lim TH, Lee SB, et al. 2014. Fabrication and operating characteristics of a flat tubular segmented-in-series solid oxide fuel cell unit bundle. *Energy* 72:215–221
[59] Fujita K, Somekawa T, Horiuchi K, Matsuzaki Y. 2009. Evaluation of the redox stability of segmented-in-series solid oxide fuel cell stacks. *Journal of Power Sources* 193:130–135
[60] Fujita K, Somekawa T, Hatae T, Matsuzaki Y. 2011. Residual stress and redox cycling of segmented-in-series solid oxide fuel cells. *Journal of Power Sources* 196:9022–9026
[61] An YT, Ji MJ, Hwang HJ, Choi BH. 2015. Fabrication of a flat tubular segmented-in-series solid oxide fuel cell using decalcomania paper. *Fuel Cells* 15:566–570
[62] Pillai MR, Gostovic D, Kim I, Barnett SA. 2007. Short-period segmented-in-series solid oxide fuel cells on flattened tube supports. *Journal of Power Sources* 163:960–965
[63] Kim YB, Ahn SJ, Moon J, Kim J, Lee H. 2006. Direct-write fabrication of integrated planar solid oxide fuel cells. *Journal of Electroceramics* 17:683–687
[64] Pi SH, Lee SB, Song RH, Lee JW, Lim TH, et al. 2013. Novel ag–glass composite interconnect materials for anode-supported flat-tubular solid oxide fuel cells operated at an intermediate temperature. *Fuel Cells* 13:392–397
[65] Yun UJ, Lee JW, Lee SB, Lim TH, Park SJ, et al. 2012. Fabrication and operation of tubular segmented-in-series (SIS) solid oxide fuel cells (SOFC). *Fuel Cells* 12:1099–1103
[66] Miyamoto K, Mihara M, Oozawa H, Hiwatashi K, Tomida K, et al. 2015. Recent progress of SOFC combined cycle system with segmented-in-series tubular type cell stack at MHPS. *ECS Transactions* 68:51
[67] Mehran MT, Khan MZ, Song RH, Lim TH, Naqvi M, et al. 2023. A comprehensive review on durability improvement of solid oxide fuel cells for commercial stationary power generation systems. *Applied Energy* 352:121864
[68] Koi M, Yamashita S, Matsuzaki Y. 2007. Development of segmented-in-series cell-stacks with flat-tubular substrates. *ECS Transactions* 7:235
[69] Cui D, Ji Y, Chang C, Wang Z, Xiao X, et al. 2020. Influence of structure size on voltage uniformity of flat tubular segmented-in-series solid oxide fuel cell. *Journal of Power Sources* 460:228092
[70] Fan J, Shi J, Zhang R, Wang Y, Shi Y. 2023. Numerical study of a 20-cell tubular segmented-in-series solid oxide fuel cell. *Journal of Power Sources* 556:232449
[71] Jamil SM, Othman MHD, Rahman MA, Jaafar J, Ismail AF, et al. 2015. Recent fabrication techniques for micro-tubular solid oxide fuel cell support: a review. *Journal of the European Ceramic Society* 35:1–22
[72] Suzuki T, Yamaguchi T, Fujishiro Y, Awano M. 2006. Improvement of SOFC performance using a microtubular, anode-supported SOFC. *Journal of The Electrochemical Society* 153:A925
[73] Suzuki T, Hasan Z, Funahashi Y, Yamaguchi T, Fujishiro Y, et al. 2009. Impact of anode microstructure on solid oxide fuel cells. *Science* 325:852–855
[74] Suzuki T, Funahashi Y, Yamaguchi T, Fujishiro Y, Awano M. 2009. Effect of anode microstructure on the performance of micro tubular SOFCs. *Solid State Ionics* 180:546–549
[75] Sin YW, Galloway K, Roy B, Sammes NM, Song JH, et al. 2011. The properties and performance of micro-tubular (less than 2.0mm O.D.) anode supported solid oxide fuel cell (SOFC). *International Journal of Hydrogen Energy* 36:1882–1889
[76] Calise F, Restucccia G, Sammes N. 2010. Experimental analysis of micro-tubular solid oxide fuel cell fed by hydrogen. *Journal of Power Sources* 195:1163–1170
[77] Sun JJ, Koh YH, Choi WY, Kim HE. 2006. Fabrication and characterization of thin and dense electrolyte-coated anode tube using thermoplastic coextrusion. *Journal of the American Ceramic Society* 89:1713–1716
[78] Rahman AHME, Kim M, Kim JH, Lee BT. 2010. Fabrication of seven cells in single tubular solid oxide fuel cell using multi-pass extrusion process. *Ceramics International* 36:1577–1580
[79] Mani B, Tavakolinia HA, Moghadam RB. 2017. A new design for co-extrusion dies: fabrication of multi-layer tubes to be used as solid oxide fuel cell. *Journal of Science: Advanced Materials and Devices* 2:425–431
[80] Zhang X, Jin Y, Li D, Xiong Y. 2021. A review on recent advances in micro-tubular solid oxide fuel cells. *Journal of Power Sources* 506:230135
[81] Tan X, Liu S, Li K. 2001. Preparation and characterization of inorganic hollow fiber membranes. *Journal of Membrane Science* 188:87–95
[82] Wei CC, Li K. 2008. Yttria-stabilized zirconia (YSZ)-based hollow fiber solid oxide fuel cells. *Industrial & Engineering Chemistry Research* 47:1506–1512
[83] Altan T, Timurkutluk C, Onbilgin S, Timurkutluk B. 2023. Novel concept of bolt-microtubular geometry for solid oxide fuel cells. *Journal of Power Sources* 576:233243
[84] Kim C, Jang I. 2024. Comprehensive review and future perspectives: 3D printing technology for all types of solid oxide cells. *Journal of Physics: Energy* 6:032003
[85] Droushiotis N, Doraswami U, Kanawka K, Kelsall GH, Li K. 2009. Characterization of NiO–yttria stabilised zirconia (YSZ) hollow fibres for use as SOFC anodes. *Solid State Ionics* 180:1091–1099
[86] Othman MHD, Wu Z, Droushiotis N, Kelsall G, Li K. 2010. Morphological studies of macrostructure of Ni–CGO anode hollow fibres for intermediate temperature solid oxide fuel cells. *Journal of Membrane Science* 360:410–417
[87] Chen L, Yao M, Xia C. 2014. Anode substrate with continuous porosity gradient for tubular solid oxide fuel cells. *Electrochemistry Communications* 38:114–116
[88] Yang C, Jin C, Chen F. 2010. Micro-tubular solid oxide fuel cells fabricated by phase-inversion method. *Electrochemistry Communications* 12:657–660

[89] Wang B, Li T, Xiao R, Hartley UW, Ueda M, et al. 2023. Study on the 4-channel micro-monolithic design with geometry control for reversible solid oxide cell. *Separation and Purification Technology* 315:123732

[90] Li T, Wu Z, Li K. 2015. Co-extrusion of electrolyte/anode functional layer/anode triple-layer ceramic hollow fibres for micro-tubular solid oxide fuel cells–electrochemical performance study. *Journal of Power Sources* 273:999−1005

[91] Kikuta K, Yasue K, Suzuki M, Kanehira S, Kirihara S. 2016. Design and fabrication of micro close end tubular SOFC with internal conduction layer. *Journal of the Ceramic Society of Japan* 124:360−364

[92] Huang W, Finnerty C, Sharp R, Wang K, Balili B. 2017. High-performance 3D printed microtubular solid oxide fuel cells. *Advanced Materials Technologies* 2:1600258

[93] Ren C, Gan Y, Yang C, Lee M, Dong G, et al. 2017. Fabrication and characterization of high performance intermediate temperature alumina substrate supported micro-tubular SOFCs. *Journal of The Electrochemical Society* 164:F722

[94] Suzuki T, Funahashi Y, Yamaguchi T, Fujishiro Y, Awano M. 2007. Fabrication of micro-tubular SOFC stack using ceramic manifold. *ECS Transactions* 7:477

[95] Suzuki T, Funahashi Y, Yamaguchi T, Fujishiro Y, Awano M. 2008. Development of cube-type SOFC stacks using anode-supported tubular cells. *Journal of Power Sources* 175:68−74

[96] Funahashi Y, Shimamori T, Suzuki T, Fujishiro Y, Awano M. 2009. New fabrication technique for series-connected stack with micro tubular SOFCs. *Fuel Cells* 9:711−716

[97] Funahashi Y, Suzuki T, Fujishiro Y, Shimamori T, Awano M. 2009. 200 W module design using micro tubular SOFCs. *ECS Transactions* 25:195

[98] Zhang R, Wang Y, Shi J, Shi Y. 2023. Design and fabrication of an easily assembled anode supported microtubular SOFC stack. *ECS Transactions* 111:851

[99] Lin C, Kerscher F, Spliethoff H. 2025. Thermal gradient management in solid oxide fuel cells: mechanisms, strategies, and future directions. *Journal of Power Sources* 656:238017

[100] Liang B, Yao Y, Guo J, Yang H, Liang J, et al. 2022. Propane-fuelled microtubular solid oxide fuel cell stack electrically connected by an anodic rectangular window. *Applied Energy* 309:118404

[101] Liu J, Wang C, Yao Y, Ye H, Liu Y, et al. 2024. Double conductive Ni-pads for a kW-class micro-tubular solid oxide fuel cell stack. *Journal of Power Sources* 591:233843

[102] Ye H, Ma Y, Wang C, Liu J, Liu Y, et al. 2023. A 3D printed redox-stable interconnector for bamboo-like tubular solid oxide fuel cells. *International Journal of Hydrogen Energy* 48:34979−34986

[103] Atrex, Ascend Energy. 2017. Atrex, Ascend Energy demonstrate ATV with SOFC range-extender. *Fuel Cells Bulletin* 2017:3−4

[104] Jaspers BC, Kuo PC, Amladi A, van Neerbos W, Aravind PV. 2021. Negative CO_2 Emissions for transportation. *Frontiers in Energy Research* 9:626538

[105] Shen M. 2021. Solid oxide fuel cell-lithium battery hybrid power generation system energy management: a review. *International Journal of Hydrogen Energy* 46:32974−32994

[106] Heidary H, El-Kharouf A, Steinberger-Wilckens R, Bozorgmehri S, Salimi M, et al. 2023. Life cycle assessment of solid oxide fuel cell vehicles in a natural gas producing country; comparison with proton electrolyte fuel cell, battery and gasoline vehicles. *Sustainable Energy Technologies and Assessments* 59:103396

[107] Meadowcroft AD, Howroyd S, Kendall K, Kendall M. 2013. Testing micro-tubular SOFCs in unmanned air vehicles (UAVs). *ECS Transactions* 57:451

[108] Bessekon Y, Zielke P, Wulff AC, Hagen A. 2019. Simulation of a SOFC/battery powered vehicle. *International Journal of Hydrogen Energy* 44:1905−1918

[109] Ultra Electronics USSI. 2018. Ultra Electronics USSI wins SOFC contract for UAS platforms. *Fuel Cells Bulletin* 2018:6−7

[110] Bahari M, Rostami M, Entezari A, Ghahremani S, Etminan M. 2022. A comparative analysis and optimization of two supersonic hybrid SOFC and turbine-less jet engine propulsion system for UAV. *Fuel* 319:123796

[111] Giacoppo G, Barbera O, Briguglio N, Cipitì F, Ferraro M, et al. 2017. Thermal study of a SOFC system integration in a fuselage of a hybrid electric mini UAV. *International Journal of Hydrogen Energy* 42:28022−28033

[112] Choudhury A, Chandra H, Arora A. 2013. Application of solid oxide fuel cell technology for power generation – a review. *Renewable and Sustainable Energy Reviews* 20:430−442

[113] Suzuki M, Takuwa Y, Inoue S, Higaki K. 2013. Durability verification of residential SOFC CHP system. *ECS Transactions* 57:309

[114] Aki H, Wakui T, Yokoyama R. 2016. Development of an energy management system for optimal operation of fuel cell based residential energy systems. *International Journal of Hydrogen Energy* 41:20314−20325

[115] George RA. 2000. Status of tubular SOFC field unit demonstrations. *Journal of Power Sources* 86:134−139

[116] Ono T, Miyachi I, Suzuki M, Higaki K. 2011. Development of residential SOFC cogeneration system. *IOP Conference Series: Materials Science and Engineering* 18:132007

[117] Suzuki M, Sogi T, Higaki K, Ono T, Takahashi N, et al. 2007. Development of SOFC residential cogeneration system at Osaka Gas and Kyocera. *ECS Transactions* 7:27

[118] Yoda M, Inoue S, Takuwa Y, Yasuhara K, Suzuki M. 2017. Development and commercialization of new residential SOFC CHP system. *ECS Transactions* 78:125

[119] Wakui T, Yokoyama R, Shimizu KI. 2010. Suitable operational strategy for power interchange operation using multiple residential SOFC (solid oxide fuel cell) cogeneration systems. *Energy* 35:740−750

[120] Pirkandi J, Ghassemi M, Hamedi MH, Mohammadi R. 2012. Electrochemical and thermodynamic modeling of a CHP system using tubular solid oxide fuel cell (SOFC-CHP). *Journal of Cleaner Production* 29−30:151−162

[121] Baniasadi E, Alemrajabi AA. 2010. Fuel cell energy generation and recovery cycle analysis for residential application. *International Journal of Hydrogen Energy* 35:9460−9467

[122] Narayanan M, Mengedoht G, Commerell W. 2021. Evaluation of SOFC-CHP's ability to integrate thermal and electrical energy system decentrally in a single-family house with model predictive controller. *Sustainable Energy Technologies and Assessments* 48:101643

[123] Yang W, Zhao Y, Liso V, Brandon N. 2014. Optimal design and operation of a syngas-fuelled SOFC micro-CHP system for residential applications in different climate zones in China. *Energy and Buildings* 80:613−622

[124] Fong KF, Lee CK. 2016. System analysis and appraisal of SOFC-primed micro cogeneration for residential application in subtropical region. *Energy and Buildings* 128:819−826

[125] Buonomano A, Calise F, d'Accadia MD, Palombo A, Vicidomini M. 2015. Hybrid solid oxide fuel cells–gas turbine systems for combined heat and power: A review. *Applied Energy* 156:32−85

[126] Park SK, Kim TS. 2006. Comparison between pressurized design and ambient pressure design of hybrid solid oxide fuel cell–gas turbine systems. *Journal of Power Sources* 163:490−499

[127] Kobayashi Y, Ando Y, Nishiura M, Kishizawa H, Iwata M, et al. 2013. Recent progress of SOFC combined cycle system with segmented-in-series tubular type cell stack at MHI. *ECS Transactions* 57:53

[128] Gandiglio M, De Sario F, Lanzini A, Bobba S, Santarelli M, et al. 2019. Life cycle assessment of a biogas-fed solid oxide fuel cell (SOFC) integrated in a wastewater treatment plant. *Energies* 12:1611

[129] Kawabata Y, Takeda D, Ochi K, Fujiki H, Oshima T, et al. 2021. Practicality evaluation of solid oxide fuel cell (SOFC) – micro gas turbine (MGT) hybrid power generation system. *Proceedings of 14th European SOFC & SOE Forum, Lucerne, Switzerland, October 20–23, 2021*, Oberrohrdorf, Switzerland: European Fuel Cell Forum. pp. 132–143 doi: 10.5281/zenodo.4550554

[130] Zhang B, Maloney D, Farida Harun N, Zhou N, Pezzini P, et al. 2022. Rapid load transition for integrated solid oxide fuel cell – gas turbine

(SOFC-GT) energy systems: a demonstration of the potential for grid response. *Energy Conversion and Management* 258:115544

[131] Lai H, Adams TA. 2023. Life cycle analyses of SOFC/gas turbine hybrid power plants accounting for long-term degradation effects. *Journal of Cleaner Production* 412:137411

[132] van Biert L, Woudstra T, Godjevac M, Visser K, Aravind PV. 2018. A thermodynamic comparison of solid oxide fuel cell-combined cycles. *Journal of Power Sources* 397:382–396

[133] Sghaier SF, Khir T, Ben Brahim A. 2018. Energetic and exergetic parametric study of a SOFC-GT hybrid power plant. *International Journal of Hydrogen Energy* 43:3542–3554

[134] Mueller F, Jabbari F, Gaynor R, Brouwer J. 2007. Novel solid oxide fuel cell system controller for rapid load following. *Journal of Power Sources* 172:308–323

[135] Mueller F, Tarroja B. 2009. High temperature stationary solid oxide fuel cell systems in the renewable future. *ASME 2009 7th International Conference on Fuel Cell Science, Engineering and Technology, June 8–10, 2009, Newport Beach, CA, USA*, ASMEDC. pp. 225–235. doi: 10.1115/FuelCell2009-85107

[136] Xi F, Ruan X, Razmjooy N. 2023. Optimal configuration and energy management for combined solar chimney, solid oxide electrolysis, and fuel cell: a case study in Iran. *Energy Sources, Part A: Recovery, Utilization, and Environmental Effects* 45:9794–9814

[137] Shariatzadeh OJ, Refahi AH, Abolhassani SS, Rahmani M. 2015. Modeling and optimization of a novel solar chimney cogeneration power plant combined with solid oxide electrolysis/fuel cell. *Energy Conversion and Management* 105:423–432

[138] Azadi P. 2012. An integrated approach for the production of hydrogen and methane by catalytic hydrothermal glycerol reforming coupled with parabolic trough solar thermal collectors. *International Journal of Hydrogen Energy* 37:17691–17700

[139] Saha AK, Chowdhury S, Chowdhury SP, Gaunt CT. 2009. Integration of wind turbine, SOFC and microturbine in distributed generation. *2009 IEEE Power & Energy Society General Meeting, July 26–30, 2009, Calgary, Canada*. IEEE. pp. 1–8 doi: 10.1109/PES.2009.5275268

[140] Hai T, El-Shafay AS, Alizadeh A, Dhahad HA, Chauhan BS, et al. 2024. Comparison analysis of hydrogen addition into both anode and afterburner of fuel cell incorporated with hybrid renewable energy driven SOFC: an application of techno-environmental horizon and multi-objective optimization. *International Journal of Hydrogen Energy* 51:1195–1207

[141] Safari A, Amini Badr A, Farrokhifar M. 2019. Modeling of integrated power system with wind turbine based on a doubly fed induction generator and solid oxide fuel cell for small-signal stability analysis. *International Transactions on Electrical Energy Systems* 29:e12119

[142] Obara S, Morel J. 2014. Microgrid composed of three or more SOFC combined cycles without accumulation of electricity. *International Journal of Hydrogen Energy* 39:2297–2312

[143] Obara S, Kawae O, Kawai M, Morizane Y. 2013. A study of the installed capacity and electricity quality of a fuel cell-independent microgrid that uses locally produced energy for local consumption. *International Journal of Energy Research* 37:1764–1783